

Carbon Nanotubes for Photovoltaics: From Lab to Industry

Laura Wieland, Han Li, Christian Rust, Jianhui Chen,* and Benjamin S. Flavel*

The use of carbon nanotubes (CNTs) in photovoltaics could have significant ramifications on the commercial solar cell market. Three interrelated research directions within the field are crucial to the ultimate success of this endeavor; 1) separation, purification, and enrichment of CNTs followed by 2) their integration into organic solar cells as a photosensitive element or 3) in silicon solar cells as a hole selective contact. All three subtopics have experienced tremendous growth over the past 20 years and certainly the performance of the silicon-based cells is now rapidly approaching that of those on industrial production lines. With a view to these three research areas, the purpose of this Progress Report is to provide a brief overview of each field but more importantly to discuss the challenges and future directions that will allow CNT photovoltaics to move out of the research lab and into end user technology. These include efforts to upscale CNT purification, improvements in power conversion efficiency, increased light absorption, the identification of new material combinations, passivation strategies, and a better understanding of charge separation and energy transfer within these systems.

and armchair nanotubes, respectively. All other nanotube conformations ($0^\circ < \theta < 30^\circ$) are referred to as being chiral. In this 1D system, circumferential electron confinement results in SWCNTs that are either metallic (m) or semiconducting (s) and the innate ability of small changes in diameter to impart large changes in the spectral position (size) of absorption maxima (bandgap) of the SWCNTs.^[1a,2] For each chiral species these maxima appear as sets of discrete excitonic transitions (S_{11} , S_{22} , S_{33} ,...etc.) in the infrared, visible, and ultraviolet and the ability to tune them with structure has made SWCNTs one of the most intensively studied nanomaterials of the past two decades.^[3]

SWCNTs meet all of the requirements for next generation technology to become flexible and potentially made entirely from carbon to aid disposal at the end of the product life-cycle. Applications for

1. Introduction


The atomic structure of a single walled carbon nanotube (SWCNT) is described by their chirality and is defined by the two integers (n,m), which describe the theoretical “roll-up” of a graphene lattice. As shown in **Figure 1a**, the integers (n,m) originate from the chiral vector, $C_h = na_1 + ma_2$, which describes the number of steps along the graphene lattice basis vectors (a_1 and a_2) in real space,^[1] and which makes an angle θ , known as the chiral angle, with the zig-zag or a_1 direction. There exist two limiting cases of 0° and 30° and these are referred to as zig-zag

SWCNTs can be found across all fields of science including photonics,^[4] telecommunications,^[5] batteries,^[6] fuel cells,^[7] high frequency transistors,^[8] biosensors,^[9] novel memory devices,^[10] molecular contacts,^[11] and cancer research.^[12] In particular, their chirality dependent bandgap, chemical stability, conductivity, and hole selectivity have made them attractive for new generation solar cells and light sensitive elements.^[13] For example, there are 200 species in the diameter range of 0.6–2 nm, which have first (S_{11}) and second (S_{22}) optical transitions ranging from 2.57 eV (visible) to 0.5 eV (near-infrared) and these already cover a majority of the solar spectrum (400–2000 nm), **Figure 1d**.^[14] Being solution-processable and fiber-shaped, CNTs can easily be integrated into different types of solar cells with distinct functions. For example, as a photoactive layer in organic solar cell, a transparent electrode in silicon and perovskite solar cells or as counter electrode in dye-sensitized solar cells.^[15] However, despite their promise, the number of real-world applications for SWCNTs in the photovoltaics (PV) industry continue to remain limited. The reasons for this are manifold and include the comparatively lower power conversion efficiency (PCE) and device area of SWCNT-based technologies, which drive simple cost-benefit arguments to retrofit existing production lines, ongoing challenges to orientate and control the structure of CNT films in a scalable manner, spurious health concerns associated with the use of CNTs^[16] and importantly, the fact that it is still not possible to selectively synthesize SWCNTs of arbitrarily defined chirality. Most synthesis methods produce a 2:1 mixture of many semiconducting and metallic chiral types and even the CoMoCAT synthesis process,^[17] which is well known to be highly enriched in small diameter (6,5), still contains at least 15 other chiral species in low concentration. Research efforts to achieve chiral specific growth are ongoing

L. Wieland, Dr. H. Li, C. Rust, Dr. J. Chen, Dr. B. S. Flavel
Institute of Nanotechnology
Karlsruhe Institute of Technology
Eggenstein-Leopoldshafen 76344, Germany
E-mail: chenjianhui@hbu.edu.cn; benjamin.flavel@kit.edu

L. Wieland, C. Rust
Institute of Materials Science
Technische Universität Darmstadt
Darmstadt 64289, Germany

Dr. J. Chen
Hebei Key Lab of Optic-Electronic Information and Materials
College of Physics Science and Technology
Hebei University
Baoding 071002, China

 The ORCID identification number(s) for the author(s) of this article can be found under <https://doi.org/10.1002/aenm.202002880>.

© 2020 The Authors. Advanced Energy Materials published by Wiley-VCH GmbH. This is an open access article under the terms of the Creative Commons Attribution License, which permits use, distribution and reproduction in any medium, provided the original work is properly cited.

DOI: 10.1002/aenm.202002880

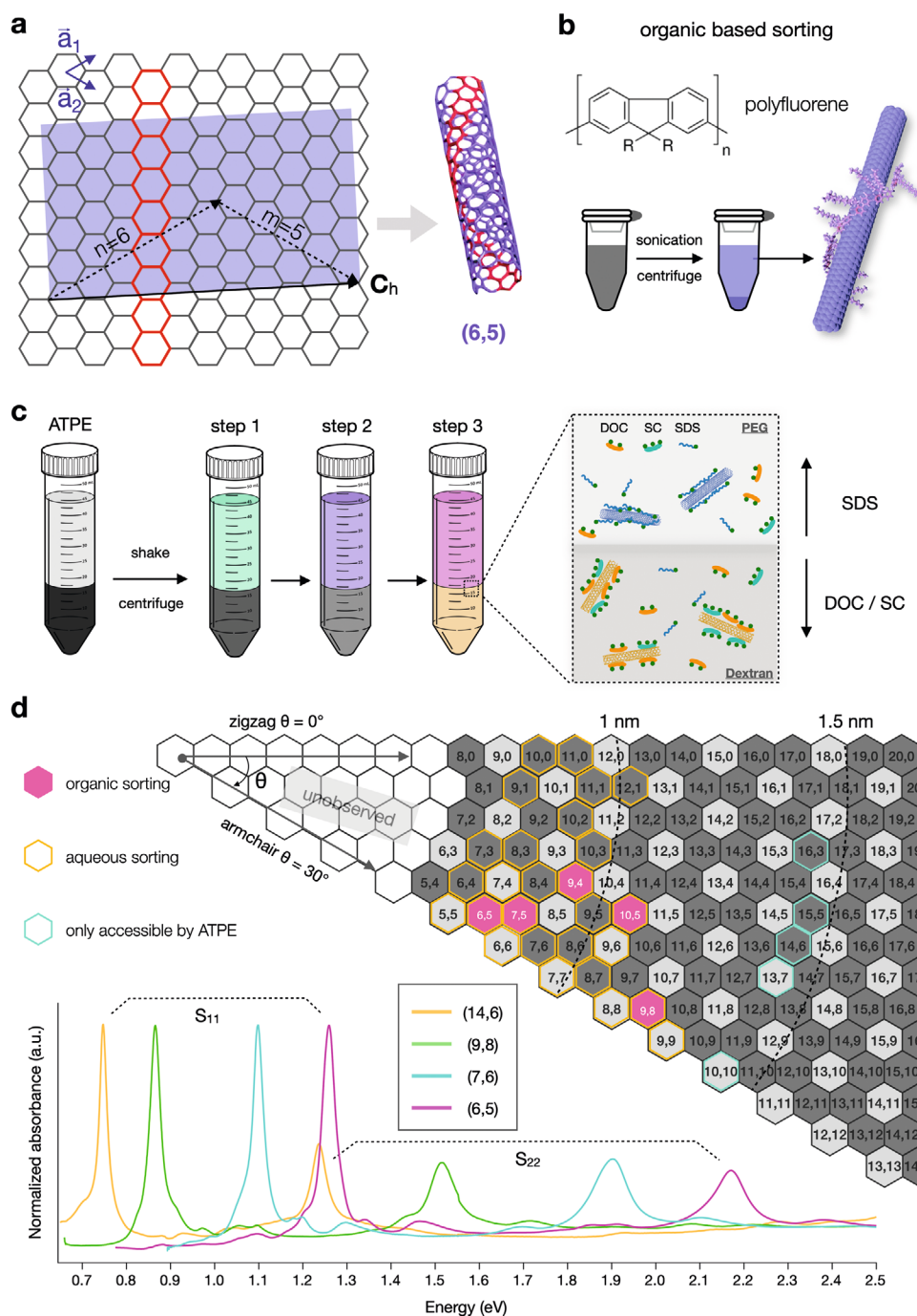


Figure 1. a) The chiral vector (C_h) describes the “roll-up” of a theoretical graphene sheet and defines the integers (n,m) . b) Extraction of chiral species using polymer wrapping in organic solvents and c) in aqueous with surfactants in a two-phase extraction process (ATPE). d) Theoretically possible (n,m) species in the diameter range 0.6–1.5 nm. Representative spectra highlight the variability of the first (S_{11}) and second (S_{22}) optical transitions for CNTs in this diameter range. The (n,m) species data are obtained from refs. [31a,34,35c,38,40].

and various approaches, including metal-catalyst free nanotube cloning of single chirality seeds,^[18] the use of bimetallic solid alloy catalysts,^[19] and bottom up synthetic strategies using carbonaceous molecular end-cap precursors^[20] have demonstrated an ability to synthesize a limited number of chiral species.^[13d]

In the research laboratory, postsynthesis separation has offered a solution to this problem, but, these are complicated techniques that are coupled to small quantities, low yields, poor

reproducibility, the use of expensive chemicals and only have easy structural selectivity to small diameter semiconducting species. Before industry can become interested in the use of a new chemical they want to ensure that it can be supplied, or at least produced repeatedly and reproducibly in large quantities. This is especially pertinent for photovoltaics due to the desire to make large area coatings and films. In order to provide the reader with a point of reference, within our research

group we typically require $\approx 4\text{--}8\ \mu\text{g}$ of (6,5) to create a 5–15 nm thick film with an area of $\approx 3.8\ \text{cm}^2$. This can be extrapolated to $\approx 0.5\ \text{mg}$ for a comparable film with an area common to the photovoltaics industry (M2+ wafer: $245.71\ \text{cm}^2$). With the exception of (6,5), the current batch size of (*n,m*) purified SWCNTs is in the sub-microgram range and it is thus difficult to engineer any new process with such a restricted supply. It is therefore becoming increasingly important that postsynthesis processing techniques consider the end point for SWCNTs as a material rather than just the isolation of pure samples. For photovoltaics, milligram scale batches are required now and there must be a realistic strategy to scale up in a cost-effective manner should it be required in the future.

In the following sections we will discuss the current capacity of leading separation techniques in terms of their yield, batch size, chiral selectivity and cost of preparation. Each technique affords (*n,m*) pure SWCNTs but we will outline differences in the quality and processability of the resultant SWCNTs and it will be seen that the material requirements for use as photosensitive elements in organic solar cells are different from those of hole selective contacts in silicon cells. In depth reviews on the topics of CNT separation^[21] the use of SWCNTs in organic photovoltaics^[2a,22] and CNT:Si heterojunctions^[12c,23] already exist. We therefore focus on the challenges and future directions for these technologies and attempt to draw a roadmap for the use of carbon nanotubes in the photovoltaics industry.

2. Separation and Purification

After two decades of development, postsynthesis purification techniques are capable of sorting the 2:1 mixture of CNT soot according to their diameter,^[24] length,^[25] wall-number,^[26] electronic property,^[27] chirality,^[28] and even enantiomeric type.^[29] Highly selective separation techniques have been developed in aqueous and organic solvents and these have facilitated many proof of principle investigations.^[2a,30] For organic photovoltaics the simplicity of the organic-based polymer extraction method has resulted in it becoming a key technology. With this method, commercially available raw soot can be combined with commercially available polyfluorene (PFO) polymers to obtain either (6,5) or (7,5) in a two-step process involving sonication or shear force mixing followed by centrifugation^[31] (Figure 1b). Despite its impressive selectivity, it is important to mention that the method cannot be arbitrarily applied to all raw soot, that it is limited to these two chiral species, that the yield of separation is low and often highly variable and that PFO is expensive. Additionally, the use of polymer extraction is contradictory to the goal of having 300+ unique (*n,m*) chiral nanotubes, with a whole array of tailorable optical and electronic properties, and this has lead researchers to search for other polymer/nanotube combinations^[31,32] but a decade of work by multiple groups has added no other bulk purifiable (*n,m*)s. Nevertheless, a polymer method, especially one involving gentle shear force mixing, is attractive because it affords long ($\approx 2\ \mu\text{m}$) SWCNTs with few defects^[31c] and an exceptionally high semiconducting content (99.99+%).^[31d,33] This means that there are fewer opportunities for exciton quenching on the SWCNT and this ensures long lifetimes and high quantum yields.

Using pricing from common chemical suppliers it is possible to make an estimate of the cost/gram of (6,5) from polymer extraction and it immediately becomes clear why this method continues to remain unattractive for industry. Using laboratory conditions, polymer wrapped (6,5) is estimated to be €36 000–73 000 per gram! Details pertaining to this calculation can be found in Figure S1 of the Supporting Information. The cost of a single large area film mentioned in the introduction would therefore be €0.29–0.58 (8 μg). Obviously, this is only an estimate and it is possible to make arguments about cost reductions associated with economies of scale and thus the real production cost being much lower, or indeed that other research groups have a better yield than us (0.025–0.05%), but it is unlikely that these will reduce the price of (6,5) to a level that is comparable to traditional organic photovoltaic materials like P3HT, C_{60} , or PC_{71}BM . These all range between €200 and 1880 per gram. Fortunately, if the issue of yield and the price of materials were to be resolved, both shear force mixing and centrifugation are highly scalable techniques for industry and this would allow for the batch size to be scaled.

By contrast, the available library of single chiral SWCNTs from aqueous based techniques far surpasses that of polymer extraction and these methods typically produce larger quantities. Figure 1d shows all of the (*n,m*) species currently isolatable by the two techniques.^[34] Notably, aqueous methods have not only been shown to separate many more semiconducting (*n,m*)s but they are also sensitive to metallic species and enantiomers.^[35] However, they are associated with a lower semiconducting content compared to polymer extraction,^[36] shorter nanotubes ($\approx 0.6\text{--}1.1\ \mu\text{m}$)^[31c] and a significantly more complex experimental method. The difficulty of aqueous methods stems from the use of surfactants like sodium dodecyl sulfate (SDS), sodium cholate (SC), or sodium deoxycholate (DOC) to disperse the raw CNT soot.^[21a,24,37] Unlike selective polymers, surfactants disperse all CNTs in the raw soot, but within these there exist small structural differences in their coating around different diameters,^[38] around the metallic and semiconducting subpopulations^[39] and to a lesser extent around (*n,m*) species or enantiomers.^[40] It is these differences in the surfactant shell which modulate the interaction of the CNTs with a third medium for separation.^[41] In early work, gel mediums such as sephacryl or agarose were shown to be highly sensitive to the variable surfactant structure around a CNT.^[40,42] Since then many groups, including our own have worked on upscaling these techniques,^[43] but, researchers have struggled with inhomogeneities in gel packing between experiments, nonspecific adsorption, and loss of nanotubes on the columns, and the need for multiple steps and columns.^[40] In a related direction, Hersam and co-workers^[27] have shown that density gradient ultracentrifugation (DGU) is sensitive to differences in the surfactant coating around a CNT by taking advantage of the different buoyant density of (*n,m*) species. Certainly, the (*n,m*) selectivity of DGU is comparable to gel-based techniques but the absence of an immobile phase (gel) to which nanotubes can adsorb is a clear advantage. However, DGU is typically performed on small volume rotors and the marginal difference in surfactant coating around each (*n,m*) species requires the highly controlled layering of race layers and an extended centrifugation time (hours). Despite protracted discussion between the different

sides as to which method is better the reality is that all of these techniques are reliant upon one highly expensive component (gels or density gradient mediums) and time has proven that the reproducibility and throughput of these techniques is not sufficient to bring chirality sorted CNTs into an industrial setting and each suffer large losses of raw material.

In our opinion, a possible solution to these problems came in 2013 when Khripin and co-workers^[44] introduced the aqueous two-phase extraction (ATPE) process. This method has since proven to be rapid, highly sensitive, and like DGU does not require a stationary phase. ATPE is reliant upon aqueous solutions of polyethylene glycol (PEG) and dextran (DX). These polymers are miscible for all concentrations below a two-phase coexistence curve of compositions (a so-called “tie-line”) above which they phase separate into a hydrophobic (PEG rich) top and hydrophilic (DX rich) bottom phase.^[45] Separation is then sensitively related to the different solvation energy of these two phases for CNTs^[21a] which is controlled by their surfactant coating.^[46] Similar with other aqueous-based sorting method, concentration, and competition between the surfactants determine the ATPE separation. In competition for the SWCNT surface, at equivalent surfactant concentrations it is often observed that the binding affinity follows the order $\text{DOC} > \text{SC} \gg \text{SDS}$, each of them also depending on SWCNT (n,m) type.^[47] As a reference point an SWCNT coated entirely by DOC or SC will be located in the DX phase and an SWCNT-coated entirely by SDS will be located in the PEG phase. Experimentally ATPE relies upon the sequential removal and readdition of CNT containing top or bottom phases to clean opposing phases (Figure 1c). A modulation of the SDS/DOC/SC ratio is used to control the surfactant shell around the SWCNT and thereby the phase in which they are found. Likewise, the addition of strong oxidants, reductants,^[48] salts,^[46,49] or changes in temperature and pH^[47,50] can influence SWCNT partitioning. By partitioning CNTs between the two phases followed by the removal of the phase with the undesired species, it is possible to eventually arrive at conditions (up to eight steps can be required) where only one (n,m) species is isolated in either the PEG or DX.

In principle ATPE is a highly scalable technique, with the batch size determined entirely by the size of the container used for the two phases and the mass of SWCNTs. In the laboratory an upper limit is usually defined by practical limitations to shake, extract, recombine, and centrifuge large volumes, not to mention increased interfacial trapping for high nanotube concentrations.^[46,50a] A conservative estimate for (6,5) from ATPE is \approx €8300–13 000 per gram and if pretreatment steps like rate-zonal purification or simple precentrifugation are used, this increases to \approx €12 000–24 000 per gram due to initial losses of raw soot, Figure S2 of the Supporting Information. ATPE costs \approx 8 times less than polymer extraction, but it is still far from being a cheap process and this is primarily associated with the high cost of dextran and DOC. Species such as (8,3) or (9,4) from ATPE from the CoMoCAT raw soot can be estimated at \approx €94 000–147 000 per gram. Here the high cost is predominantly related to the expense of the raw soot and the low concentration of target (n,m) species within it.

For an industrial application it is important to resolve the increased experimental involvement of ATPE relative to polymer wrapping. The separation of (6,5) described in Figure S2 of

the Supporting Information requires \approx 2 h of laboratory work, despite the actual separation including centrifugation occurring within 5 min. This is due to the requirement of having to remove the top and bottom phases carefully by hand, adjustment of surfactant concentration at each step and multiple steps. Removal by hand is acceptable for proof-of-principle experiments but it is unlikely to be acceptable for industry. Counter current chromatography and the closely related technique of centrifugal partition chromatography offer a realistic solution and remove the need for user interaction and can perform cascade separations sequentially and inline. These techniques are based on continuous liquid–liquid phase partitioning and are capable of performing all steps including mixing, centrifugation and extraction of the two phases in an automated flow through manner. For this reason they are already being used in the separation of natural products,^[51] biological products,^[13a,52] and enantiomers^[53] by the chemical and pharmaceutical industries and recently, Zhang et al.^[54] and Knight et al.^[55] performed preliminary experiments on SWCNTs. Although there are still many issues with the use of these techniques, including the high viscosity of the two-phase components and low stationary phase retention which leads to low separation purity,^[54] this single-step process looks promising to provide industrial-scale single chirality (n,m) species in the future. Industrial systems capable of handling well over 1 L of solution already exist and this would place the processable batch size to 1 g raw soot and would provide 200 mg of (6,5) in one run!

3. Carbon Nanotubes in Organic Solar Cells

Organic solar cells with CNTs in the photoactive layer commonly use s-SWCNTs as an electron donor in combination with C_{60} or fullerene-derivates as the acceptor to form a type II heterojunction. Exciton dissociation at their interface drives solar energy conversion and this requires a minimum energy known as the thermodynamic driving force (ΔG).^[22a] ΔG is defined as the difference between the ionization potential of the donor (IP_D) and the electron affinity of the acceptor (EA_A) minus a component associated with the exciton self-energy, which can be calculated from the electronic bandgap (E_{el}) of the CNT minus the exciton binding energy (E_b). $\Delta G = |\text{IP}_D - \text{EA}_A| - [E_{el} - E_b]$.^[22] Characteristic exciton binding energies for carbon nanotubes range from 0.2–0.5 eV.^[56] Exciton dissociation occurs only if the net driving energy is greater than zero and this concept is often simplified to be the energetic offset between the lowest unoccupied molecular orbitals (LUMOs) of the donor and acceptor.^[13a] Alternatively, s-SWCNTs have also been used as an electron acceptor in combination with materials such as poly(3-hexylthiophene-2,5-diyl) (P3HT) or poly(3-octylthiophene) (P3OT).^[12d,57]

SWCNT-based solar cells have almost exclusively been fabricated in bilayer stacks between an indium tin oxide (ITO) substrate and metals like silver or aluminum (Figure 2a).^[58] Carrier selective layers such as poly(3,4-ethylenedioxythiophene):poly(styrenesulfonate) (PEDOT:PSS),^[12b,58c] bathocuproine,^[58a] or MoO_3 ^[58b,59] are also usually used to aid charge separation. Researchers have been motivated by the goal to use the chirality dependent optical properties of a SWCNT to match the solar

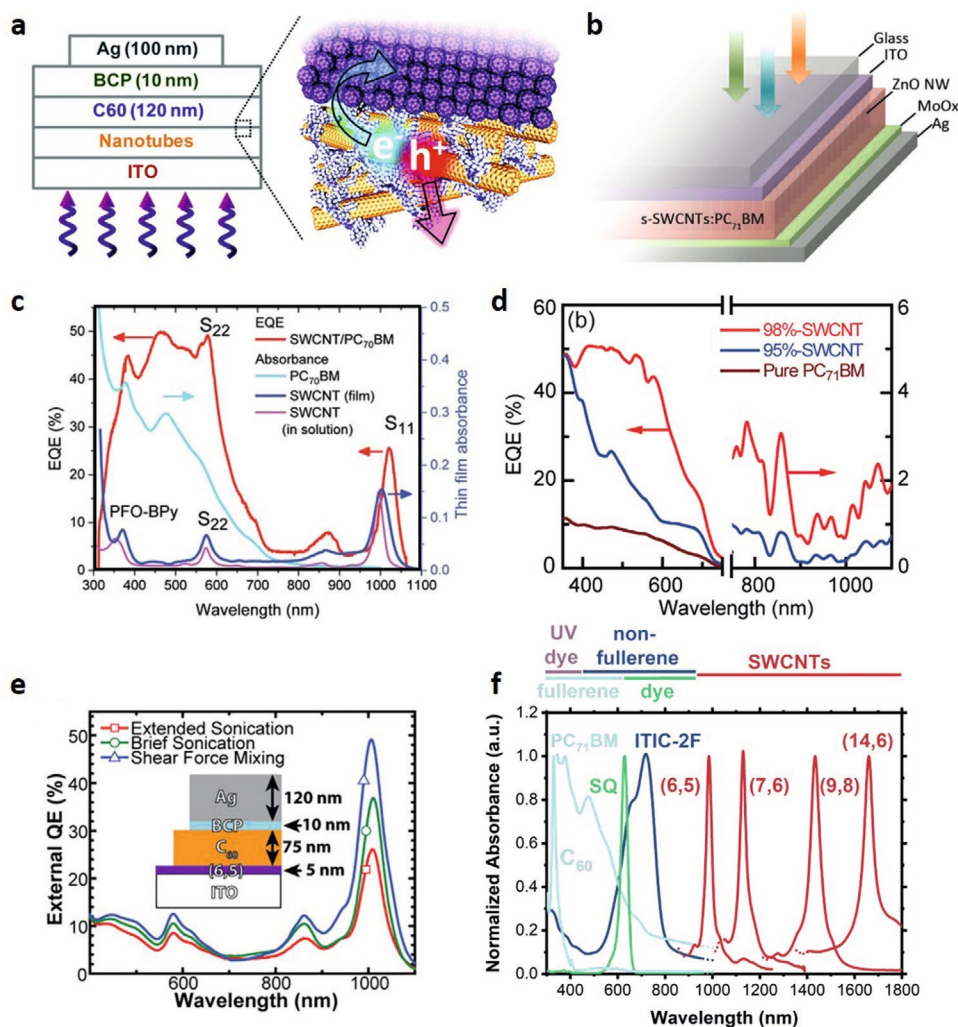


Figure 2. Typical organic solar cell architectures where the CNTs is either a) a thin film^[58a] or b) used in a blend.^[58b] EQE measurements from leading c) thin film ((6,5)/PC₇₁BM)^[58c] and d) blended (P3HT s-SWCNT/PC₇₁BM) architectures.^[58b] e) Variation of EQE ((6,5)/C₆₀) with the nanotube dispersion technique^[68b] and f) absorption spectra of commonly used, or suggested, components for these solar cells. Reproduced with permission.^[58a] Copyright 2011, American Chemical Society. Reproduced with permission.^[58b] Copyright 2014, American Chemical Society. Reproduced with permission.^[58c] Copyright 2018, John Wiley & Sons.

spectrum,^[4c,58a,60] and early simulations by Tune and Shapter^[61] have predicted the possibility of broadband light absorption. The authors simulated the light harvesting ability of mono- and polychiral films and found that a mixture of (6,4), (9,1), (7,3), and (7,5) can collect up to 28% of the AM1.5 solar spectrum. Likewise, work by Arnold et al.^[2a] has predicted that a 150 nm thick film of 10 small diameter s-SWCNTs (0.8–1.4 nm) would be capable of absorbing 86% of the solar spectrum up to 1200 nm. However, as discussed later, the practical use of polychiral samples or thick films is complicated by energy transfer within the film^[62] and trapping in small diameter species, along with a significant fraction of the generated excitons ending up in dark nonradiative states.^[63] Most investigations have therefore targeted single chiral films of (6,5) or (7,5) and an example external quantum efficiency (EQE) measurement is shown in Figure 2c.^[58c]

In closely related devices, s-SWCNTs have also been blended with polymers such as poly(3-hexylthiophene-2,5-diyl) (P3HT).^[57a] In this direction, researchers have capitalized upon existing

organic photovoltaic material combinations (i.e., P3HT/PC₇₁BM) and the goal has been to push their performance by extending light absorption in the infrared (IR).^[58b,59,64] SWCNT/fullerene blends are rarely prepared.^[65] Figure 2b shows a leading example from the Hersam group, in which zinc oxide nanowires are additionally used as an electron transport layer.^[58b] These also interpenetrate the active layer to minimize the collection length and reduce variations in layer morphology.^[58b,59,64] A representative EQE measurement is shown in Figure 2d. In this design, incident photons up to 700 nm are absorbed by P3HT (peak at 440 nm^[66]) and PC₇₁BM (peak at 400–750 nm^[58c]) and an EQE of 50% is reached. The IR (800–1100 nm), contribution from the SWCNTs is markedly lower, with maximum EQEs of about 3% achieved. Nevertheless, broad light absorption in the visible has led this polychiral blend to be current PCE record holder for the field at 3.2%.^[59] Unsurprisingly, the ability to increase PCE by increasing light collection from CNT unrelated components has not escaped

the rest of the field. For the SWCNT/fullerene bilayer cells, those made with PC₇₁BM^[58c,67] are likewise also generally more efficient than those from C₆₀^[60b,68] due to broader light absorption (Figure 2f). For example, (6,5)/PC₇₁BM cells from Classen et al.^[58c] have reached PCEs of 2.9%, despite EQE from the SWCNTs remaining at 26%, which is lower than the 43% in the work by Shea and Arnold^[60b] with (6,5)/C₆₀ who only reported a PCE of 1.02%. The device area of these headline solar cells is 1.2 mm² for the SWCNT-P3HT/PC₇₁BM blend^[59] and 2.0 mm² for work of Classen et al.^[58c] The (6,5)/PC₇₁BM cells were also upscaled to 10.4 mm² and a PCE of 2.7% achieved.

For organic solar cells, high performance is related to SWCNTs with a high semiconducting purity, and those which are low in defect content and long (1.1 μm) in order to avoid exciton quenching.^[68b] As described previously, PFO derivatives and shear force mixing have been exceptionally successful in this regard.^[31c,33a,69] The use of organic solvents also simplifies film formation and dispersions can be deposited directly on the device with spin-coating,^[58c] doctor blading,^[58a] or ultrasonic spraying.^[70] With the exception of the SWCNT-P3HT blends, where P3HT aids dispersion of the CNTs and a dichlorobenzene solution facilitates spin-coating the use of aqueous dispersions has been considerably more difficult and device performance much lower. Material incompatibilities have meant that films from aqueous dispersions must usually be prepared separately and laminated onto the device by either dissolving a membrane^[71] or through wet-transfer processes.^[12a,13a] Examples include, Jain et al.^[71a] who prepared a 100 nm filtered film in a (6,5)/C₆₀ device with PCE of 0.10%, or similar work from our group, where a super thin (6,5) layer prepared by evaporation driven self-assembly was used and a PCE of 0.14% for a 10.5 mm² area were achieved.^[12b,13a] Isborn et al.^[72] have also dispersed s-SWCNTs and C₆₀ in a water/methanol mixture using graphene nanoribbons (GNR), which allowed for 7–10 nm thick layers to be electrospayed and final (6,5)-C₆₀-GNR/PC₆₁BM cells achieved a PCE of 1.14%.

The type of residual species left on the nanotube sidewall are also very different for aqueous and organic dispersions and these play an important role in energy transfer, exciton lifetime, and finally the overall performance of the solar cell. For aqueous dispersions, the surfactants can usually be washed away with water and pristine films of CNTs obtained, albeit it should be mentioned that complete removal of the membrane or transfer agent is often difficult to ensure. For organic dispersions a minimum polymer content is required to disperse the CNTs and this ends up in the assembled device. The exception to this is work by Joo et al.^[73] who developed an unwrapping method by selective chelation of BPy to remove the PFO-BPy in a post treatment process. Despite initial concerns that residual polymer content might be detrimental to performance, it actually turns out to enhance the excitonic lifetime by shielding the nanotube from the surrounding environment.^[62c,68a,74] Polymer wrapped SWCNTs have exciton lifetimes of ≈1 ps, whereas ATPE-purified SWCNTs are closer to ≈300 fs^[62a,75] and efficient solar cells require long excitonic lifetimes to ensure maximum exciton migration to the donor-acceptor interface.^[2a,62a,75] Bilayer solar cells achieve this via exciton transfer at nanotube crossing points. Nevertheless, the absence of polymer

also results in strongly coupled SWCNTs, which enables rapid downhill energy transfer to the smallest bandgap SWCNT, and this can trap excitons and impede transfer between larger majority chiralities.^[62c]

On the issue of the dispersion technique itself, aqueous dispersions are almost exclusively prepared via ultrasonication whereas shear force mixing (SFM) is becoming increasingly common popular for polymer wrapped dispersions.^[31c,63,68b] Recently, the Arnold group showed that energy transfer in s-SWCNT films prepared by SFM is 20% more efficient than those of sonicated samples.^[63] The longer, pristine nanotubes from SFM improved the probability that an exciton will transfer to the next SWCNT rather than finding a defect site and becoming trapped. This improves interfiber hopping and increases exciton diffusion to the interface. By preparing solar cells from PFO-BPy wrapped (6,5) exposed to different degrees of harshness in their dispersion; extended and brief ultrasonication and shear force mixing, they were able to show an improvement in FF and V_{oc} for the SFM sample, Figure 2e.^[68b] EQE from the CNTs also depends on the defect density^[76] and exciton lifetime, and the SFM sample achieved 49% (4.2 ps) compared to 38% (3.0 ps) and 28% (2.1 ps) for the brief or extended sonication samples, respectively.^[68b]

Regardless of the specific steps involved to manufacture a film, the necessity of excitons created within that film to traverse a considerable distance to the interface is a significant drawback of the bilayer design.^[12b,77] Obviously, thicker films would absorb more light, create more excitons, and thus lead to more efficient solar cells but if most of those excitons never lead to free carriers, then thicker films are not beneficial. In fact, this effect can already be seen upon comparison of the work by Jain et al.^[71a] using a 100 nm (6,5) film to that by us with a 2–3 nm thick film.^[12b,13a] Except for the thicker film and the hole transport layer PEDOT:PSS in our stack the two devices are identical, but both obtained PCEs of ≈0.1%. An optimum thickness clearly exists and this is defined by the exciton diffusion length in SWCNT films. Using ultrafast spectroscopy^[62a,78] or photocurrent measurements in bilayer devices the exciton diffusion length has been determined to be 5–10 nm.^[58a,60a,62a] For reference the exciton diffusion length in C₆₀ is ≈5 nm.^[77a] As such, the EQE at the SWCNTs and J_{sc} of the device linearly increase with SWCNT film thickness until 5–15 nm is reached and an abrupt decrease is observed.^[60,68b] Consequently, all high performance SWCNT/fullerene solar cells consist of SWCNT films of only a few nanometers.^[13a,60b,65] Fortunately, Bindl et al.^[58a] have predicted that a 4 nm thick film is enough to approach internal quantum efficiency of 100%. Experimentally, C₆₀ thickness of 30–120 nm are used.^[13a,60b,65,70] Although this is much thicker than the exciton diffusion length in C₆₀, it is an approach used to smooth out inhomogeneities in the SWCNT film, and more importantly to optimize the electric field intensity within the layer stack such that it is matched to the physical position of the SWCNTs within the device and their optical transitions using transfer matrix calculations.^[13a,70,76]

Complications associated with the short exciton diffusion length in the photoactive layers are certainly not unique to SWCNT solar cells. The broader organic photovoltaics community has been faced with this problem for decades and has thus developed the bulk heterojunction to address it.^[79] In

these architectures, morphology control is essential and inefficient intermixing of the donor/acceptor and the formation of large domains will only further hinder exciton dissociation.^[80] For an SWCNT/fullerene blend the 1D structure and stiffness of the CNTs make the morphology of these blends difficult to control.^[2a] Furthermore, solvent systems capable of simultaneously dispersing SWCNTs and C₆₀ in high concentration are rare.^[65,72] The (6,5)/PC₇₁BM bulk heterojunctions by Classen et al.^[58c] therefore suffered reductions in J_{sc} and FF (1.91 mA cm⁻² and 0.33) compared to the bilayers.

An alternate solution is the pre-formation of an aerogel and the subsequent interpenetration of either donor or acceptor within these. In this direction, Ye et al.^[81] have already prepared an SWCNT aerogel by cocasting a mixture of PMMA and s-SWCNTs in chlorobenzene followed by the removal of the PMMA with acetone. PC₇₁BM was then infiltrated within the aerogel and solar cells with $V_{OC} = 0.56$ V, $J_{sc} = 7.2$ mA cm⁻², FF = 0.41, and PCE = 1.7% with a 100 nm thick active layer were obtained. Importantly, PCE and J_{sc} were found to increase for SWCNT thickness up to 100 nm. Although these results are encouraging, the sacrificial matrix approach is limited by the possibility of PMMA residues.^[60a] Chemical cross-linking of the nanotubes to form an aerogel may offer a solution to this problem. The Schaffer group have used p-Diiodobenzene to covalently link the sidewalls of unsorted CNTs followed by critical point drying to form an aerogel.^[82] Cross-linking has the added benefit of enhanced structural integrity of the SWCNT aerogel,^[83] and the same chemistry can be used to lock fullerenes in place.^[84] However, an increased I_D/I_G ratio after cross-linking suggests that this comes at the expense of increased trap sites for the excitons. Setaro et al.^[85] provide a solution to this problem and have shown that the use of azidodichloro-triazine as cross-linker is capable of preserving the π -conjugation of the CNTs.

Toward increasing the light absorption of SWCNT solar cells by using other (*n,m*) species, mixtures thereof or indeed large diameter species it is necessary to find new acceptor molecules. With view to the discussion on thermodynamic driving force, ΔG , C₆₀ has a LUMO at -4.05 eV and SWCNTs vary from -3.65 eV for (6,5) to -4.04 eV for larger diameter species (1.8 nm).^[12b] The requirement of ΔG for exciton dissociation therefore places an upper limit on the nanotube diameter at ≈ 1 nm for C₆₀.^[12b] This corresponds to roughly 20 possible species and the internal quantum efficiency (IQE) for (*n,m*) species approaching this limit decreases.^[12b,58a,67] Larger diameters require acceptors with higher electron affinity. Modification of C₆₀ is the obvious route and Ihly et al.^[86] prepared a series of fullerenes with various electron withdrawing groups to tune the electron affinity. In their work, laser vaporized SWCNTs, mainly (11,9), showed the best electron transfer yield in combination with C₆₀(CF₃)₄. Nonfullerene acceptors including perylene diimide based acceptors or ITIC-4F have also been investigated recently by Wang et al.^[67] Bilayer devices from small and large diameter nanotubes were prepared but the highest IQE (50%) was still for the smallest of nanotubes (0.78 nm). This is despite literature suggesting LUMO positions of -4.14 to -4.19 eV for these acceptors,^[87] which in theory should better match a diameter of 1.4 nm. This discrepancy may be explained by cyclic voltammetry measurements placing the LUMO position of ITIC-4F at

-3.99 eV, but the authors also point out that very little is known about these heterojunctions and that nonfullerene acceptors with higher electron affinity are still required.^[88]

In a related direction, endohedral filling of the SWCNTs with dye molecules may further extend the light harvesting capability of these solar cells, and photoinduced energy transfer from the organic dye to the s-SWCNTs has already been observed with PL and photocurrent spectroscopy.^[89] Molecules including quaterthiophene (4T),^[90] squarylium dye (SQ),^[89a,91] p,p'-dimethylaminonitrostilbene (DANS),^[92] and ferrocenylthiocarbonyl based dyes^[93] have all been placed inside a SWCNT. However, these all require a minimum diameter of SWCNT (≈ 1.1 nm),^[91,92] known as the sieving diameter, which places them outside the diameter range accessible to C₆₀ as an acceptor. Furthermore, whilst dye filling will increase the visible/UV light absorption of the nanotube, it is important to remember that large diameter SWCNTs in combination with nonfullerene acceptors would already capture most of the incident light in the visible and IR regions. As shown in Figure 2f, ITIC-2F already absorb light between 550 and 800 nm.^[87c] The additional effort to fill an SWCNT is thus only beneficial when it extends the light absorption of the combined active layers and not just the SWCNT. Dyes with absorption bands in the UV would complement SWCNT/NFA cells, whilst (6,5)/C₆₀ cells require dyes in the visible but their small diameter prohibits encapsulation.

3.1. Future of Carbon Nanotubes in Thin Film Photovoltaics

Despite being a convenient system to study excitonic and energy transfer processes within carbon nanotubes themselves, it is hard to envisage that their use as light sensitive elements, at least under the constraints of current designs, will become an industrially attractive technology in the near future. It is possible to argue that CNTs will find their niche in infrared sensing, but it is difficult to argue why competing solar cell technologies such as perovskites, copper indium gallium selenide (CIGS), cadmium telluride (CdTe), and organic solar cells, which have achieved PCE values of 18–25%,^[94] should be replaced by CNTs. There are still too many challenges that need to be addressed before organic CNT solar cells are able to compete with these systems. Primarily these are associated with improvements in the light absorption of the solar cells and the correspondingly low efficiency. It must become possible to use the entire range of s-SWCNTs (small and large diameter) and strategies to reduce excitonic trapping in mixtures of (*n,m*) species are required. The rapidly growing field of nonfullerene acceptors should in principle provide a solution to the first problem, but these remain expensive and to date have not been shown to enable the use of any chiral species not already accessible with C₆₀. For this reason, and taking into consideration difficulties to completely isolate different (*n,m*) species from each other in a film, the use of thick single chiral films in the form of an aerogel in a bulk-heterojunction design is attractive. These will help to overcome the short exciton diffusion length in SWCNTs and the increased optical density of the absorption tail located left and right of the central maximum will increase overall absorption. Ideally the aerogel will have pores sizes similar to the exciton diffusion length and cross-links between

the individual CNTs and/or acceptors should offer the best efficiency in terms of architectural considerations. In light of the high performance of the aforementioned thin film technologies, it will also be important to continue research on blended systems. Certainly, because these are built on established materials combinations, they have a much higher probability of reaching competitive PCEs. In truth, perhaps the most sensible way to utilize CNTs as a light sensitive element is to extend the light absorbed by other materials into the infrared rather than struggling to harvest broadband light with a narrow absorber.

Alternatively, narrow absorption bands and the tailorable electronic property of SWCNTs are advantageous for use as transparent conductive electrodes^[22b,95] or hole transport layers. Examples of these can already be found for perovskite,^[86,96] CIGS,^[97] CdTe,^[98] and organic solar cells.^[99] In organic solar cells, P3HT-dispersed SWCNTs used as a hole transport layer achieved a PCE of 7% for PTB7/PC₇₁BM and this is comparable to cells with PEDOT:PSS.^[100] In CIGS solar cells the CNTs replace the ZnO transparent oxide and in CdTe solar cells they are the semitransparent back contact. These cells have achieved PCEs of 12.4% and 13% PCE, respectively.^[97,98] Improved hole extraction has also been demonstrated for perovskite solar cells by introducing an SWCNT interlayer between the perovskite and the hole transport layer spiro-MeTAD.^[101] Replacing spiro-MeTAD with P3HT-dispersed SWCNTs and PMMA or polycarbonate lead to PCEs of \approx 13%.^[96a] Likewise, an aerosol-synthesized SWCNT film as transparent electrode infiltrated by spiro-MeTAD approached a PCE of 16%^[102] and acid treated double walled carbon nanotubes exceeded 17.2%.^[23a] Recently, undoped SWCNT hole transport layers coupled with PMMA or undoped spiro-MeTAD have enabled stable 17.4% or 20% PCE perovskite solar cells^[103] and Jeon et al. have shown that triflic acid doped CNTs as transparent electrodes outperform the metal counterpart in a perovskite solar cell with 18.8% and 18.4% PCE achieved.^[104] Flexible perovskite solar cells, made with SWCNTs^[105] on both sides of the device have also been demonstrated and these pave the way to industrial processes like roll-to-roll fabrication.

4. Carbon Nanotubes in Silicon Photovoltaics

Si-wafer-based solar cells currently dominate the global PVs market and they have done so now for roughly three decades. Their high PCE, high-stability, long-lifetime, and a scalability of the steps required for their fabrication have led to the development of a product with a high performance/cost ratio and an estimated market share > 90%.^[106] Despite rapid advances in competing and emerging fields (perovskites, organics, and CIGS solar cells^[107]), continued process refinement and new cell architectures have allowed silicon to persist as the leading photovoltaic technology. These include a series of high-efficiency designs from the early aluminum back surface field (Al-BSF) cell^[108] to the recently industrialized passivated emitter and rear cell (PERC)^[109] and in the future to the scaled silicon heterojunction (SHJ) and interdigitated back contact (IBC or HJ-IBC) cells.^[110] High-quality surface passivation strategies and carrier selective contacts^[106] have played a key role in their development and cutting-edge research cells (HJ-IBC) achieve power conversion efficiencies of 26.7%.^[94e]

These high PCEs are very close to the theoretical maximum of 29.4%,^[111] but, each new design has been coupled with an increase in complexity. Dielectric passivation schemes with SiO₂,^[112] Al₂O₃,^[113] SiN_x,^[114] and hydrogenated amorphous silicon (a-Si:H)^[115] have become increasingly important and these require high-vacuum and/or high-temperature processes for their deposition. Likewise, carrier-selective contacts require phosphorus/boron doping of bulk silicon or thin films thereof. Doping of bulk silicon is the most popular method to fabricate a p–n junction and is achieved by high-temperature diffusion or ion implant technology to form p⁺ (boron) or n⁺ (phosphorous) regions near surface of the wafer.^[116] Thin amorphous silicon films are doped by plasma enhanced chemical vapor deposition combined with toxic boron/phosphorous gas precursors.^[117] Together these steps have a negative impact on the final performance/cost ratio of the cells. As such the solar cell most commonly found on domestic rooftops is still the Al-BSF cell and this is due to its simple design and comparatively high PCE.^[118] These cells usually cost 0.21 \$/W but since 2018 they are slowly being displaced by the PERC design on industrial production lines.

Figure 3a summarizes the development of silicon photovoltaic technology from 2010 to 2020 with the associated cost and global annual production. Incremental improvements in PCE with new designs, Figure 3b, are now offset by disproportionate increases in cost, which in light of the theoretical PCE maximum creates a bottleneck for future design improvements. Research therefore focusses on two aspects; 1) breaking the theoretical limit in PCE and/or 2) reducing the fabrication cost. The former has recently been achieved by perovskite/silicon tandem cells.^[119] The later will require the development of low temperature processes and inexpensive novel materials for passivation and carrier-selective contacts. To this end research must be directed toward the replacement of the doped silicon layer with dopant free heterocontacts which can be evaporated, spin, and spray coated.^[120] These strategies should mirror the simplicity of Al paste printing used in the Al-BSF cell, but with the important exception that they should not involve a metal–semiconductor contact as this leads to recombination losses and has limited the Al-BSF design to a PCE of \approx 20%.^[106] Promising candidates to achieve this include; spin-coating of PEDOT,^[120c,121] cesium carbonate (Cs₂CO₃),^[122] MoO_x,^[123] and most recently CNTs, which form a hole selective contact to n-type silicon. Currently, due to the use of mostly unsorted raw material containing CNTs with different bandgaps and electronic types, it has been difficult to identify the physical nature of the CNT:Si junction as simply a Schottky, metal–insulator–semiconductor or p–n junction^[124] but in our work we have found that the Barden model fits the device physics well.^[124a]

Fortunately, relative to the rigid purity constraints of the organic cells, the material requirements of CNTs as a hole selective contact are much more relaxed and raw soot has even been used. These can cost as little as \approx €30 per gram. For CNT:Si solar cells, chiral selection is typically limited to raw soot and/or chiral species with optical transitions located outside the spectral range of silicon (350–1100 nm), thus maximizing light absorption by silicon, and/or to large diameter species due to their increased conductivity.^[23a,124d,125] Either way, unlike the organic cells, aqueous methods are much better suited due to

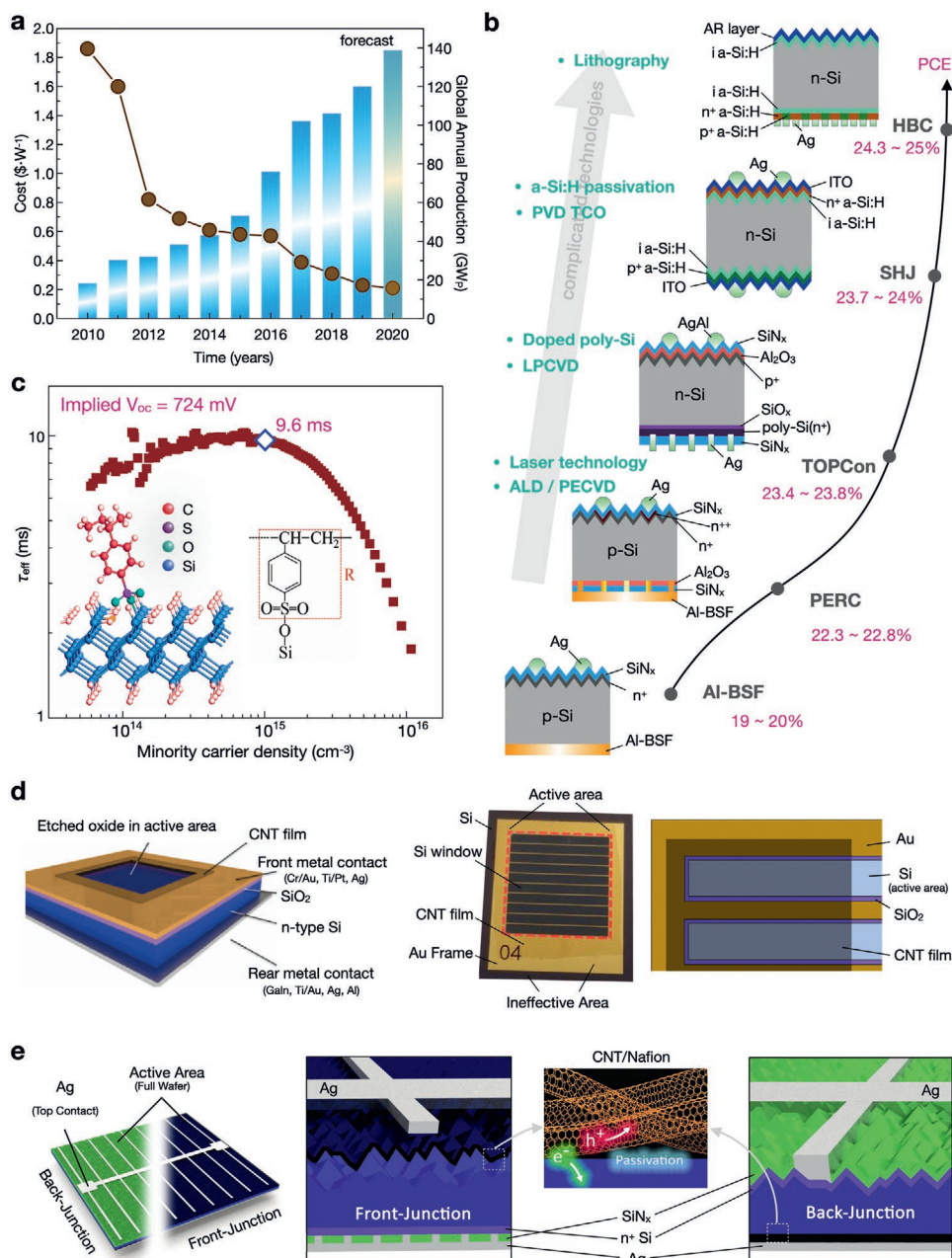


Figure 3. a) The cost (dotted line) and global production (bar chart) of silicon photovoltaics. b) The advancement of silicon photovoltaic technology to achieve high PCEs from early Al-BSF cells to current market mainstream PERC cells, transitional TOPCon cells to next-generation SHJ and HBC cells. The efficiency values shown are typical for industry at the present stage. c) The injection level dependent lifetime curves of Nafion polymer thin-film passivated n-type wafers with a resistivity of 1–5 Ω cm.^[139b] Inset shows first-principles total-energy calculations of PSS molecule grafted on the H-terminated Si surface and the schematic chemical formula of PSS.^[139a] Comparison of d) a window-like geometry to e) industry standard device geometries with a front and back design. Reproduced with permission.^[139b] Copyright 2018, American Chemical Society. Reproduced with permission.^[139a] Copyright 2017, AIP Publishing.

their pristine surface, which maximizes the CNT:Si interfacial area. A high semiconducting content has to date been shown to be less important.

Since early work by Wei et al.^[126] reporting a PCE of 1.3%, there has been significant interest in developing this technology,^[23b] but until recently PCEs have remained <17%. These low efficiencies can mostly be attributed to the solar cell design employed and this was in turn a result of technical

difficulties to integrate CNTs. In most cases, researchers employed an architecture resembling that of an organic solar cell with a window or frame like geometry defined in the middle of a silicon wafer.^[32,124d,126–127] In this geometry, a SiO₂/Si wafer is etched to reveal a small silicon opening in the SiO₂ and the surrounding SiO₂ is coated with Au, Ag, or Pt/Ti. This design was successful for many years because it allowed for the CNT film to be processed separately and later transferred

to the window. Contacts to the silicon (hole selective) and the metal (top contact) were also easily achieved and the CNT film remained the uppermost layer (front side of the cell), and this made it possible to test various chemical dopants.^[124d] Most importantly, this design facilitated the use of inherently porous CNT films and avoided metal penetration during evaporation/sputtering of the top contact (Figure 3d).

Upon comparison to Figure 3b it can be seen that this device geometry is highly unusual. No other architecture used commercially has the carrier selective contact placed above the metal top contact nor do they include a window. Fundamentally the window geometry is limited and it is unlikely that it will ever reach industrial production lines. This architecture is useful in testing new combinations of materials in the laboratory but the area is usually small ($0.008\text{--}2\text{ cm}^2$)^[23b] and it is difficult to scale up without compromising PCE. The requirement of a window also increases the ineffective area, where no light is collected, and it is not possible to perform a good wet chemical process (e.g., RCA) without removing the SiO_2 frame. These are all basic prerequisites for high-efficiency crystalline Si (c-Si) solar cells to be industrialized.^[128] More specifically, difficulties to scale up in this design are caused by the CNTs having to assume multiple roles; 1) as a hole selective layer (intended) and 2) as a transparent conductive layer (unintended).^[129] These two roles are not commensurate and the trade-off between them is captured by the $\sigma_{\text{DC}}/\sigma_{\text{OP}}$ figure of merit from Hu et al.^[130] To date, most of the improvements in the field can broadly be summarized as an optimization of the figure of merit and this has been achieved by doping the CNTs with HNO_3 ,^[131] superacid,^[127b,132] AuCl ,^[133] SOCl_2 ,^[134] $\text{CuCl}_2/\text{Cu}(\text{OH})_2$,^[124d] and Nafion.^[135] In hindsight this has developed CNT films to become closer to ITO in its function as a transparent conductive layer than as a hole selective contact. In fact, researchers have been so concerned with the figure of merit that few groups even considered interface passivation,^[136] antireflective coatings^[137] or light management,^[138] device geometry or the use of a back surface in their devices. This is a peculiar observation, especially in light of their well-established importance in the broader field of silicon photovoltaics. However, to be fair, the porosity of the CNT film once again made the use of traditional passivation layers like a-Si:H or SiN_x from CVD difficult due to adhesion problems of the seed particles and mostly research came from CNT specific laboratories.

Recently, Chen et al.^[139] developed a passivation scheme involving organic thin films that rivals traditional dielectrics^[112,140] and which most importantly is compatible with a porous CNT film.^[139b,141] The method is reliant upon spin-coating polymers with a sulfonic functional group ($-\text{SO}_3\text{H}$) and the ability of these to spontaneously form suboxides ($\text{Si}-\text{O}-\text{R}$) at the silicon surface.^[142] This solution processed passivation scheme can achieve an effective minority carrier lifetime of 9.6–28.6 ms, as shown in Figure 3c, and is in line with hydrogenated amorphous Si or SiO_2 film-passivation schemes used in the current PV industry.^[112,140] Unlike conventional chemical passivation or field-effect passivation, an electrochemical grafting passivation of silicon via electron transfer at polymer/silicon hybrid interface, is suggested to be responsible for the passivation mechanism.^[142a] The inset

in Figure 3c shows first-principles total-energy calculations of PSS molecule grafted on the H-terminated Si surface and the schematic chemical formula of PSS. Based on this electrochemical passivation, the interface state is switchable, with its features of enhanced passivation due to external conditions, such as an O_2 atmosphere or an applied bias voltage.^[143] To date, PSS,^[139a] poly(2-acrylamido-2-methylpropanesulfonic acid),^[142a] polystyrene-block-poly(ethylene-ran-butylene)-block-polystyrene-sulfonated-cross-linkable (PS-*b*-PERB),^[142a] and Nafion^[139b] have been used for this purpose. On their own, these polymers are insulating and when cast onto a porous film they work to fill the void space between the CNTs and the silicon surface. In 2020, we used this to our advantage and spin-coated Nafion onto CNT:Si solar cells. This resulted in the formation of a passivated charge selective contact (PCSC) consisting of two mixed interfacial regions; 1) a region in which carbon nanotubes contact silicon and are responsible for exciton dissociation and hole transport; 2) nanoscale silicon areas passivated by Nafion to ensure high minority carrier lifetimes. In addition to passivation, the Nafion layer also acted as an antireflective coating and nanotube dopant.^[144] The thickness of the Nafion film was tailored to ensure that the uppermost CNTs could still be electrically contacted, but by filling the voids in the film an effective physical blocking to metal penetration during electrode evaporation was also created.^[144a] This allowed us to employ solar cell architectures resembling those in Figure 3b, in which the metal contact is placed directly on top of the CNT/Nafion film.

Two industry standard device geometries were fabricated, one with a front-junction design and the other with the CNTs placed on the rear of the device (Figure 3e). Both designs allowed for the entire wafer to be used and areas of up to 16 cm^2 ^[144a] with PCEs approaching 19% were reported. Importantly, the back-junction architecture was new to the field and addressed many of the design-related challenges for carbon nanotube silicon solar cells. Namely, the CNT film no longer had a dual-purpose role as hole transport and transparent conductive layer. On the rear of the device, CNTs function solely as a hole transport layer and factors like film morphology and alignment are less important. With view to the future we believe that a back-junction design is the more appropriate way to utilize CNT in Si solar cells. Further in 2020, we combined CNTs and Nafion into a single ink that could be spin-coated in a single step and this was applied to an architecture taken directly from industrial production lines.^[106,144a] In a comparatively simple design, consisting of a phosphorous-diffused front surface field (FSF), an SiN_x antireflection layer, and a screen-printed silver grid with an H-pattern of busbars on the front, a CNT/Nafion ink were used to replace the doped junction on the rear, Figure 4a,b. A power conversion efficiency of 21.4%, an open-circuit voltage (V_{oc}) of 654 mV, a short-circuit current density (J_{sc}) of 39.9 mA cm^{-2} and a fill factor (FF) of 82% on a device area of 4.8 cm^2 were obtained. The high J_{sc} was confirmed by EQE and its integrated current density curves, Figure 4b, which is close to the EQE level of the SHJ solar cells.^[145] An FF of 82% surpasses all previous work for CNT-Si heterojunction solar cells, while being a record for dopant-free contact architectures, including hole-selective MoO_x and PEDOT based Si solar

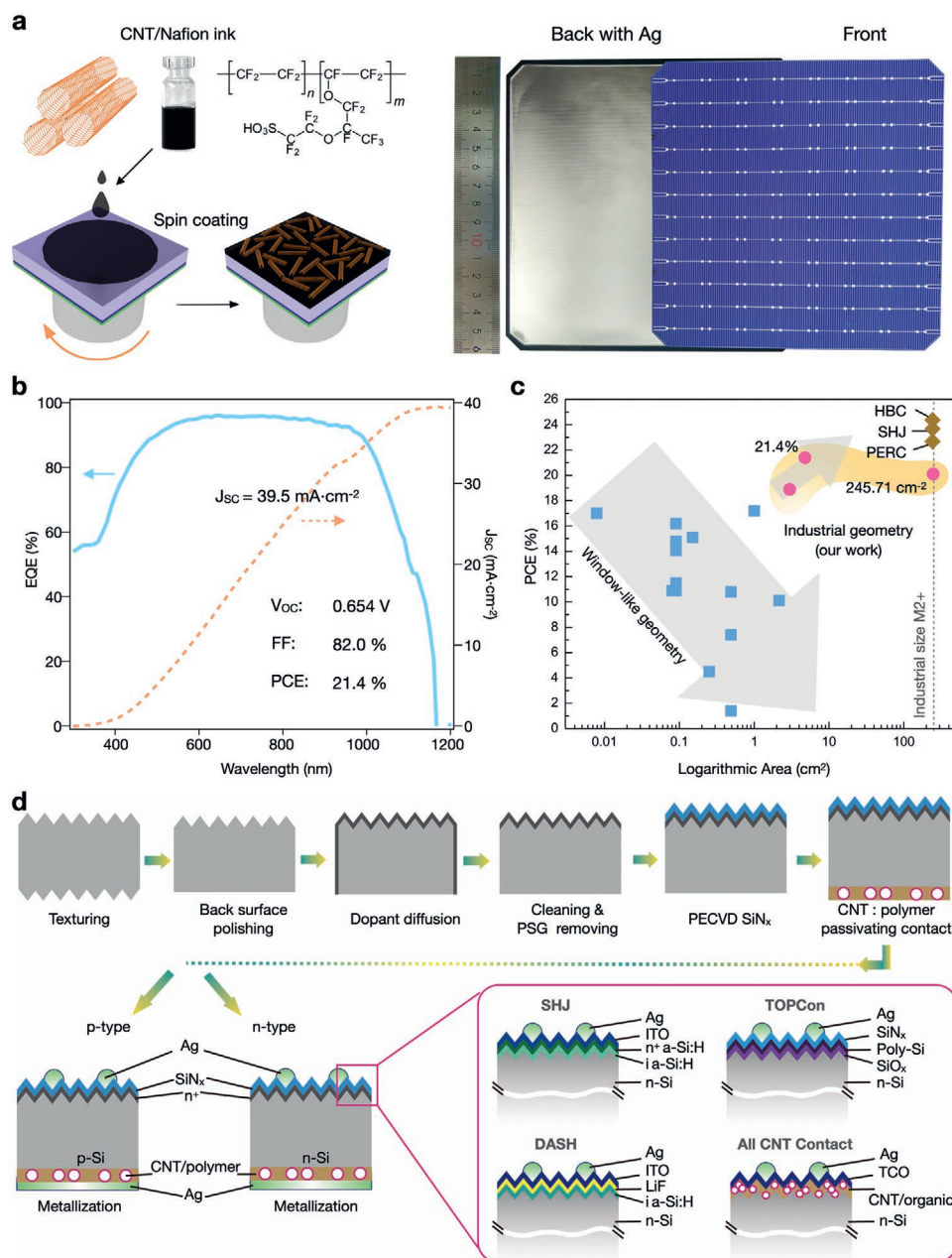


Figure 4. a) The combination of CNTs and Nafion to afford a PCSC ink that can be spin-coated onto the back of large area (245.71 cm²) silicon solar cells.^[144a] b) EQE of this device and performance values. c) Comparison of PCE values obtained using window-like and industrial geometries. d) A roadmap to achieve higher efficiencies with CNT:silicon photovoltaics.

cells.^[123c,146] We speculated that the high FF was related to the CNTs themselves and that it was a result of their higher carrier mobility.^[147] Due to the work function difference between p-type CNTs and n-type silicon a built-in potential is established and the use of dopants only further enhances the work function of the CNTs and band bending at the interface. For example, in our work, Nafion doping altered the work function of the CNT film from 4.6 eV (undoped) to 5.1 eV and this corresponded to an enhancement of built-in potential from 0.41 to 0.7 V.^[141b] A PCE of 20.1% was obtained on an industrial size (245.71 cm²) wafer. Currently this is the largest area

and highest performance achieved by a CNT:Si solar cell and compares favorably to the boron doped and dielectric passivated n-type silicon cell in the same design (PCE: 21.08%, V_{oc} : 661 mV J_{sc} : 39.43 mA cm⁻²) but has the important advantage of not requiring high temperatures or vacuum equipment. This suggests that the combination of low-dimensional materials with an organic passivation will be a new strategy to high performance photovoltaics. A unique benefit to the use of CNTs is their tunable band structure, which may lead to further improvements in built-in potential, especially at the CNT:Si interface, in the future.

4.1. Roadmap for CNTs in Silicon Photovoltaics

Toward the real-world application of CNT:Si technology it is almost certain that future designs with improved PCE will take inspiration from the broader silicon PV field. As outlined above p-type silicon solar cells using Al-BSF technology have dominated the market for many years, but now, due to their higher efficiency, absence of light-induced degradation of the dopant and double-side electrical generation, solar cells built around n-type silicon are forecast to become the next generation main stream technology.^[148] To date, the drawback of n-type technology has always been a higher fabrication cost and longer production lines relative to the Al-BSF cell. This was primarily associated with the high temperatures required for boron diffusion to form the p⁺ emitter layer, additional wet chemical cleaning steps and the use of AgAl pastes to improve the contact between the electrode and p⁺ layer. The use of a PCSC in the form of a CNT:Nafion ink already dramatically reduces the complexity of fabrication and allows for all of the benefits of n-type solar cells to be obtained with a close to p-type process (Figure 4d). In a very simplistic design, fabrication of cells from both types of silicon can consist of only six main steps: silicon surface texturing; front dopant diffusion to yield the FSF followed by SiN_x deposition; screening printing of the front fingers; CNT:Nafion coating, and Ag metallization on the back. In the simplest examples, the single-step deposition of a CNT:Nafion layer is analogous to a-Si:H(p)/a-Si:H(i) or SiN_x/Al₂O₃/c-Si(p⁺) layer stacks, which are commonly used as the emitter of n-type silicon solar cells.

Clearly, the front of the device is still prepared with industrially standardized processes, but, it is precisely here where we predict the next developments for CNT:Si solar cells to occur. Several possibilities for future designs are highlighted in Figure 4d. Despite the relatively high PCE of our work,^[144a] previous cells employed an FSF comprised of a diffused phosphorous n⁺ region with an SiN_x layer for passivation.^[144a] In this homo-FSF design, direct metal–silicon contact and imperfect SiN_x passivation limit the final obtainable V_{oc}.^[106] A better scheme is to adopt the SHJ design, where typically a ITO/a-Si:H(n⁺)/a-Si:H(i) layer stack is used as a passivating contact. In principle, the SHJ design avoids carrier recombination at the metal contacts, but the large absorption coefficient of a-Si:H means that even a few nanometers have significant parasitic photon absorption and lead to reductions in current (J_{sc}).^[123a] In a tunnel oxide passivated contact (TOPCon) design the amorphous silicon layer is replaced by wide bandgap SiO₂, but the phosphorous doped polycrystalline layer still contributes to high free carrier absorption at long wavelength.^[149] In an even more advanced architecture, wider bandgap materials such as LiF, TiO₂, and TiON^[120a,128a,150] can be selected and the doped silicon layers replaced by dopant free asymmetric heterocontacts (DASH cell).^[151] Although these cells are dopant free, they are still reliant upon thin intrinsic amorphous silicon and suffer parasitic absorption. Nevertheless, using these three relatively simple improvements on the front we predict PCEs of ≈23% for CNT:Si cells. The ultimate advancement of the DASH concept will be to develop n-type CNT inks to complement the existing p-type inks and these will allow for truly low temperature and cheap CNT(p)/n-Si/CNT(n⁺) cells to be

built. However stable n-type dopants for the CNTs are rare^[152] and finding one that can simultaneously disperse the CNTs in analogy to Nafion will be challenging. Additionally, this architecture reintroduces issues associated with light absorption by the CNT film on the front and the necessity to use (n,m) pure CNTs to avoid it. In this regard the number of studies on truly chiral pure samples is limited and use of mixed chirality films, dopants and a poorly defined interface has precluded precise determination of the junction physics and operating principle behind CNT:Si solar cells.^[124c,141b,153] It may still be possible to achieve V_{oc} enhancements using (n,m) pure samples that have an appropriate band alignment to silicon. Rear metallization is also still a cost contributor, whether that is to deposit Ag or Al, and the use of Ag nanowire inks or low temperature metal pastes designed by Zielke et al.^[154] may offer an alternative in the future. These completely omit vacuum equipment and high-temperature processes. But ideally it is best to have a transparent conductive layer on rear of the cells to take advantage of double-side electric generation. Here the material strategy could be carbon-based materials like graphene or CNTs,^[155] especially small diameter metallic CNTs, due to their long wavelength transmittance.

As with all PV technologies, stability is an important consideration and the CNT:Si heterojunction cells are no exception. Several research groups have reported long term stable devices.^[127a,136,156] However, in all cases the PCE was below 20% and accelerated stability testing such as 80 C/80 RH for high performance devices (>20%) is still lacking. In the roadmap provided above the CNTs are considered to be a stable material and the main problem for device stability is associated with the organic passivation strategy. For organic materials the inclusion of oxygen and water usually affect the device performance and stability mainly depends on exposure to the atmosphere. As a dopant, Nafion is regarded to be very stable or even permanent^[157] with the sheet resistance of Nafion doped SWCNT films shown to be unchanged for more than 600 days. This has allowed for Nafion doped devices to maintain a constant PCE for more than 120 days.^[136] On the other hand, the surface passivation afforded by Nafion when exposed to ambient conditions was found to be stable for only a period of hours and continued to degraded over several days.^[142a] This was ascribed to the hygroscopic nature of the Nafion layer. In a related work, Chen et al.^[142a] showed that the stability of a sulfonic group based passivation scheme can be increased to 430 days with the use of an ALD-Al₂O₃ encapsulation layer. It is expected that after final encapsulation of the CNT:Si cells and incorporation into a module by the photovoltaics industry that the issues surrounding stability can be solved but it will be a challenging target going forward.

5. Conclusion

Carbon nanotubes are a versatile material with multiple potential functions for photovoltaics. In principle, all elements of a solar cell, from the light sensitive component to carrier selective contacts, layers for passivation and transparent conducting films can be replaced by carbon nanotubes and their composites. Advanced processing techniques have seen the yield

and purity of single chiral species increase dramatically and it is now possible to realistically consider their application to industry. However, the high cost of chirality pure CNTs, regardless of the separation method used, does continue to make them somewhat of an exotic material. For this reason, the development of growth methods with a chiral preference will continue to be important, but, it is unlikely that it will ever be possible to selectively grow all chiral species. In an industrial setting, growth and separation will thus continue to be synergistic rather than one being a solution for the other. Due to the high yield, lower cost, and ability to access many more chiral species, aqueous methods certainly seem the better choice for large area coatings, but it is imperative that the quality of the resultant nanotubes reaches that of organic techniques. This includes the carbon nanotube length, semiconducting content, defect level, control over the ingress of ions or water and the development of simple film formation techniques.

In order for the industrial uptake of carbon nanotubes to occur they must find their niche because they are faced with strong competition from alternative materials and/or photovoltaic designs. As a photosensitive element in organic solar cells, the low efficiency of these devices on their own currently precludes their direct use and this is despite high efficiency in the infrared. In view of the success of tandem silicon/organic or silicon/perovskite solar cells, perhaps the future will be witness to the use of organic-CNT solar cells on the rear of these cells or indeed in a tandem architecture with CNT:Si cells. These would certainly take advantage of the unique infrared peaks of the CNTs and lead to highly efficient devices. However, current matching between the two cells will be difficult and will require a twofold increase from the organic-CNT cell and thus significantly thicker CNT films. Unless the difficulties to achieve thicker films can be resolved, the varying optical properties of CNTs may therefore be more useful in organic solar cells as a tailorable transparent hole selective contact or conductive electrode rather than the absorber. Certainly, as a hole selective contact in silicon photovoltaics, devices are approaching performance values which are competitive with current industrial cells and a clear roadmap toward even higher efficiencies has been provided. Without doubt a solution processable passivation scheme is highly attractive and enables the use of porous nanomaterial networks. Although, before these cells can become truly relevant it is imperative that stability issues associated with the use of Nafion are resolved, either through advanced encapsulation strategies or the use of replacement materials such as sulfonated poly(ether ether ketone). The use of carbon nanotubes in a passivated charge selective contact scheme will also need to be offset against other 1D and 2D materials, such as flakes of graphene, black phosphorous or MoS₂, which have also been shown to form an extended porous network and act as carrier selective contacts. Nevertheless, the future use of CNTs in photovoltaics appears to be bright and the barriers to application are diminishing rapidly.

Supporting Information

Supporting Information is available from the Wiley Online Library or from the author.

Acknowledgements

B.S.F. gratefully acknowledges support from the Deutsche Forschungsgemeinschaft (DFG) under Grant Nos. FL 834/2-1, FL 834/2-2, FL 834/5-1, and FL 834/7-1. J.C. gratefully acknowledges support from the China Scholarship Council, National Natural Science Foundation of China (Grant No. 61804041) and Outstanding Youth Science Foundation of Hebei province (Grant No. F2019201367).

Open access funding enabled and organized by Projekt DEAL.

Conflict of Interest

The authors declare no conflict of interest.

Keywords

chirality, energy, silicon, solar cells, SWCNT

Received: September 9, 2020

Revised: October 27, 2020

Published online: November 12, 2020

- [1] a) M. S. Dresselhaus, G. Dresselhaus, R. Saito, *Carbon* **1995**, *33*, 883; b) T. W. Odom, J.-L. Huang, P. Kim, C. M. Lieber, *Nature* **1998**, *391*, 62; c) T. W. Odom, J.-L. Huang, P. Kim, C. M. Lieber, *J. Phys. Chem. B* **2000**, *104*, 2794; d) M. S. Dresselhaus, G. Dresselhaus, A. Jorio, *Annu. Rev. Mater. Res.* **2004**, *34*, 247.
- [2] a) M. S. Arnold, J. L. Blackburn, J. J. Crochet, S. K. Doorn, J. G. Duque, A. Mohite, H. Telg, *Phys. Chem. Chem. Phys.* **2013**, *15*, 14896; b) T. W. Ebbesen, P. M. Ajayan, *Nature* **1992**, *358*, 220.
- [3] A. Jorio, G. Dresselhaus, M. S. Dresselhaus, *Carbon Nanotubes*, Springer, Berlin **2008**.
- [4] a) P. Avouris, M. Freitag, V. Perebeinos, *Nat. Photonics* **2008**, *2*, 341; b) F. Pyatkov, V. Fütterling, S. Khasminkaya, B. S. Flavel, F. Hennrich, M. M. Kappes, R. Krupke, W. H. P. Pernice, *Nat. Photonics* **2016**, *10*, 420; c) M. Engel, K. E. Moore, A. Alam, S. Dehm, R. Krupke, B. S. Flavel, *ACS Nano* **2014**, *8*, 9324.
- [5] S. Tatsuuru, M. Furuki, Y. Sato, I. Iwasa, M. Tian, H. Mitsu, *Adv. Mater.* **2003**, *15*, 534.
- [6] B. J. Landi, M. J. Ganter, C. D. Cress, R. A. DiLeo, R. P. Raffaele, *Energy Environ. Sci.* **2009**, *2*, 638.
- [7] A. Varga, M. Pfohl, N. A. Brunelli, M. Schreier, K. P. Giapis, S. M. Haile, *Phys. Chem. Chem. Phys.* **2013**, *15*, 15470.
- [8] M. Steiner, M. Engel, Y.-M. Lin, Y. Wu, K. Jenkins, D. B. Farmer, J. J. Humes, N. L. Yoder, J.-W. T. Seo, A. A. Green, M. C. Hersam, R. Krupke, P. Avouris, *Appl. Phys. Lett.* **2012**, *101*, 053123.
- [9] J. Wang, *Electroanal* **2005**, *17*, 7.
- [10] B. S. Flavel, J. Yu, J. G. Shapter, J. S. Quinton, *J. Mater. Chem.* **2007**, *17*, 4757.
- [11] C. Thiele, H. Vieker, A. Beyer, B. S. Flavel, F. Hennrich, D. M. Torres, T. R. Eaton, M. Mayor, M. M. Kappes, A. Golzhauser, H. V. Lohneisen, R. Krupke, *Appl. Phys. Lett.* **2014**, *104*, 103102.
- [12] a) X. Yu, B. Munge, V. Patel, G. Jensen, A. Bhirde, J. D. Gong, S. N. Kim, J. Gillespie, J. S. Gutkind, F. Papadimitrakopoulos, J. F. Rusling, *J. Am. Chem. Soc.* **2006**, *128*, 11199; b) M. Pfohl, K. Glaser, J. Ludwig, D. D. Tune, S. Dehm, C. Kayser, A. Colsmann, R. Krupke, B. S. Flavel, *Adv. Energy Mater.* **2016**, *6*, 1501345; c) D. D. Tune, F. Hennrich, S. Dehm, M. F. G. Klein, K. Glaser, A. Colsmann, J. G. Shapter, U. Lemmer, M. M. Kappes, R. Krupke, B. S. Flavel, *Adv. Energy Mater.* **2013**, *3*, 1091; d) D. J. Bindl, N. S. Safron, M. S. Arnold, *ACS Nano* **2010**, *4*, 5657.

- [13] a) M. Pfohl, K. Glaser, A. Graf, A. Mertens, D. D. Tune, T. Puerckhauer, A. Alam, L. Wei, Y. Chen, J. Zaumseil, A. Colsmann, R. Krupke, B. S. Flavel, *Adv. Energy Mater.* **2016**, *6*, 1600890; b) S. Qiu, K. Wu, B. Gao, L. Li, H. Jin, Q. Li, *Adv. Mater.* **2019**, *31*, 1800750; c) M. C. Hersam, *Nat. Nanotechnol.* **2008**, *3*, 387; d) B. Liu, F. Wu, H. Gui, M. Zheng, C. Zhou, *ACS Nano* **2017**, *11*, 31.
- [14] a) R. B. Weisman, S. M. Bachilo, *Nano Lett.* **2003**, *3*, 1235; b) M. Pfohl, D. D. Tune, A. Graf, J. Zaumseil, R. Krupke, B. S. Flavel, *ACS Omega* **2017**, *2*, 1163.
- [15] a) X. M. Fu, H. Sun, S. L. Xie, J. Zhang, Z. Y. Pan, M. Liao, L. M. Xu, Z. Li, B. J. Wang, X. M. Sun, H. S. Peng, *J. Mater. Chem. A* **2018**, *6*, 45; b) T. Chen, L. B. Qiu, Z. B. Cai, F. Gong, Z. B. Yang, Z. S. Wang, H. S. Peng, *Nano Lett.* **2012**, *12*, 2568; c) G. Z. Guan, Z. B. Yang, L. B. Qiu, X. M. Sun, Z. T. Zhang, J. Ren, H. S. Peng, *J. Mater. Chem. A* **2013**, *1*, 13268; d) Z. B. Yang, M. K. Liu, C. Zhang, W. W. Tjiu, T. X. Liu, H. S. Peng, *Angew. Chem., Int. Ed.* **2013**, *52*, 3996; e) Z. B. Yang, L. Li, H. J. Lin, Y. F. Luo, R. X. He, L. B. Qiu, J. Ren, H. S. Peng, *Chem. Phys. Lett.* **2012**, *549*, 82.
- [16] a) S. F. Hansen, A. Lennquist, *Nat. Nanotechnol.* **2020**, *15*, 3; b) D. A. Heller, P. V. Jena, M. Pasquali, K. Kostarelos, L. G. Delogu, R. E. Meidl, S. V. Rotkin, D. A. Scheinberg, R. E. Schwartz, M. Terrones, *Nat. Nanotechnol.* **2020**, *15*, 164.
- [17] B. Kitiyanan, W. Alvarez, J. Harwell, D. Resasco, *Chem. Phys. Lett.* **2000**, *317*, 497.
- [18] Y. Yao, C. Feng, J. Zhang, Z. Liu, *Nano Lett.* **2009**, *9*, 1673.
- [19] F. Yang, X. Wang, D. Zhang, J. Yang, Z. Xu, D. Luo, J. Wei, J.-Q. Wang, Z. Xu, F. Peng, X. Li, R. Li, Y. Li, M. Li, X. Bai, F. Ding, Y. Li, *Nature* **2014**, *510*, 522.
- [20] J. R. Sanchez-Valencia, T. Dienel, O. Groning, I. Shorubalko, A. Mueller, M. Jansen, K. Amsharov, P. Ruffieux, R. Fasel, *Nature* **2014**, *512*, 61.
- [21] a) M. Zheng, *Top. Curr. Chem.* **2017**, *375*, 13; b) K. E. Moore, D. D. Tune, B. S. Flavel, *Adv. Mater.* **2015**, *27*, 3105.
- [22] a) J. L. Blackburn, *ACS Energy Lett.* **2017**, *2*, 1598; b) T. A. Shastry, M. C. Hersam, *Adv. Energy Mater.* **2017**, *7*, 1601205.
- [23] a) I. Jeon, Y. Matsuo, S. Maruyama, *Single-Walled Carbon Nanotubes*, Springer, Berlin **2019**, p. 271; b) D. D. Tune, B. S. Flavel, *Adv. Energy Mater.* **2018**, *8*, 1703241.
- [24] M. S. Arnold, S. I. Stupp, M. C. Hersam, *Nano Lett.* **2005**, *5*, 713.
- [25] X. Huang, R. S. McLean, M. Zheng, *Anal. Chem.* **2005**, *77*, 6225.
- [26] K. E. Moore, M. Pfohl, F. Hennrich, V. S. K. Chakradhanula, C. Kuebel, M. M. Kappes, J. G. Shapter, R. Krupke, B. S. Flavel, *ACS Nano* **2014**, *8*, 6756.
- [27] M. S. Arnold, A. A. Green, J. F. Hulvat, S. I. Stupp, M. C. Hersam, *Nat. Nanotechnol.* **2006**, *1*, 60.
- [28] M. Zheng, A. Jagota, E. D. Semke, B. A. Diner, R. S. Mclean, S. R. Lustig, R. E. Richardson, N. G. Tassi, *Nat. Mater.* **2003**, *2*, 338.
- [29] X. Wei, T. Tanaka, T. Hirakawa, Y. Yomogida, H. Kataura, *J. Am. Chem. Soc.* **2017**, *139*, 16068.
- [30] a) M. C. Gwinner, F. Jakubka, F. Gannott, H. Sirringhaus, J. Zaumseil, *ACS Nano* **2012**, *6*, 539; b) S. Khasminkaya, F. Pyatkov, B. S. Flavel, W. H. Pernice, R. Krupke, *Adv. Mater.* **2014**, *26*, 3465.
- [31] a) A. Nish, J.-Y. Hwang, J. Doig, R. J. Nicholas, *Nat. Nanotechnol.* **2007**, *2*, 640; b) S. Liang, H. Li, B. S. Flavel, A. Adronov, *Chem. - Eur. J.* **2018**, *24*, 9799; c) A. Graf, Y. Zakharko, S. P. Schiessl, C. Backes, M. Pfohl, B. S. Flavel, J. Zaumseil, *Carbon* **2016**, *105*, 593; d) S. K. Samanta, M. Fritsch, U. Scherf, W. Gomulya, S. Z. Bisri, M. A. Loi, *Acc. Chem. Res.* **2014**, *47*, 2446.
- [32] F. Wang, D. Kozawa, Y. Miyauchi, K. Hiraoka, S. Mouri, Y. Ohno, K. Matsuda, *Nat. Commun.* **2015**, *6*, 6305.
- [33] a) K. S. Mistry, B. A. Larsen, J. L. Blackburn, *ACS Nano* **2013**, *7*, 2231; b) L. Liu, J. Han, L. Xu, J. Zhou, C. Zhao, S. Ding, H. Shi, M. Xiao, L. Ding, Z. Ma, *Science* **2020**, *368*, 850.
- [34] a) J. A. Fagan, C. Y. Khripin, C. A. Silvera Batista, J. R. Simpson, E. H. Hároz, A. R. Hight Walker, M. Zheng, *Adv. Mater.* **2014**, *26*, 2800; b) X. Tu, S. Manohar, A. Jagota, M. Zheng, *Nature* **2009**, *460*, 250; c) F. Jakubka, S. P. Schießl, S. Martin, J. M. Englert, F. Hauke, A. Hirsch, J. Zaumseil, *ACS Macro Lett.* **2012**, *1*, 815; d) R. Si, L. Wei, H. Wang, D. Su, S. H. Mushrif, Y. Chen, *Chem. Asian J.* **2014**, *9*, 868.
- [35] a) X. Tu, A. R. Hight Walker, C. Y. Khripin, M. Zheng, *J. Am. Chem. Soc.* **2011**, *133*, 12998; b) A. A. Green, M. C. Duch, M. C. Hersam, *Nano Res.* **2009**, *2*, 69; c) H. Li, G. Gordeev, O. Garrity, N. A. Peyyety, P. B. Selvasundaram, S. Dehm, R. Krupke, S. Cambré, W. Wenseleers, S. Reich, *ACS Nano* **2020**, *14*, 948; d) G. Ao, J. K. Streit, J. A. Fagan, M. Zheng, *J. Am. Chem. Soc.* **2016**, *138*, 16677; e) X. Wei, T. Tanaka, Y. Yomogida, N. Sato, R. Saito, H. Kataura, *Nat. Commun.* **2016**, *7*, 12899; f) X. Wei, T. Tanaka, T. Hirakawa, M. Tsuzuki, G. Wang, Y. Yomogida, A. Hirano, H. Kataura, *Carbon* **2018**, *132*, 1; g) K. E. Moore, M. Pfohl, D. D. Tune, F. Hennrich, S. Dehm, V. S. K. Chakradhanula, C. Kubel, R. Krupke, B. S. Flavel, *ACS Nano* **2015**, *9*, 3849.
- [36] a) L. Wei, B. S. Flavel, W. Li, R. Krupke, Y. Chen, *Nanoscale* **2017**, *9*, 11640; b) G. S. Tulevski, A. D. Franklin, A. Afzali, *ACS Nano* **2013**, *7*, 2971.
- [37] H. Li, G. Gordeev, S. Wasserroth, V. S. K. Chakradhanula, S. K. C. Neelakandhan, F. Hennrich, A. Jorio, S. Reich, R. Krupke, B. S. Flavel, *Nat. Nanotechnol.* **2017**, *12*, 1176.
- [38] J. A. Fagan, E. H. Hároz, R. Ihly, H. Gui, J. L. Blackburn, J. R. Simpson, S. Lam, A. R. Hight Walker, S. K. Doorn, M. Zheng, *ACS Nano* **2015**, *9*, 5377.
- [39] T. A. Shastry, A. J. Morris-Cohen, E. A. Weiss, M. C. Hersam, *J. Am. Chem. Soc.* **2013**, *135*, 6750.
- [40] H. Liu, D. Nishide, T. Tanaka, H. Kataura, *Nat. Commun.* **2011**, *2*, 309.
- [41] J. G. Clar, C. A. Silvera Batista, S. Youn, J.-C. J. Bonzongo, K. J. Ziegler, *J. Am. Chem. Soc.* **2013**, *135*, 17758.
- [42] K. Moshhammer, F. Hennrich, M. M. Kappes, *Nano Res.* **2009**, *2*, 599.
- [43] a) H. P. Liu, T. Tanaka, Y. Urabe, H. Kataura, *Nano Lett.* **2013**, *13*, 1996; b) A. M. Goja, H. Yang, M. Cui, C. Li, *Bioprocess. Technol.* **2013**, *4*, 1000140; c) B. S. Flavel, K. E. Moore, M. Pfohl, M. M. Kappes, F. Hennrich, *ACS Nano* **2014**, *8*, 9687; d) A. Hirano, T. Tanaka, Y. Urabe, H. Kataura, *ACS Nano* **2013**, *7*, 10285.
- [44] C. Y. Khripin, J. A. Fagan, M. Zheng, *J. Am. Chem. Soc.* **2013**, *135*, 6822.
- [45] M. Iqbal, Y. Tao, S. Xie, Y. Zhu, D. Chen, X. Wang, L. Huang, D. Peng, A. Sattar, M. A. B. Shabbir, *Biol. Proced. Online* **2016**, *18*, 18.
- [46] N. K. Subbaiyan, S. Cambré, A. N. G. Parra-Vasquez, E. H. Hároz, S. K. Doorn, J. G. Duque, *ACS Nano* **2014**, *8*, 1619.
- [47] H. Li, G. Gordeev, O. Garrity, S. Reich, B. S. Flavel, *ACS Nano* **2019**, *13*, 2567.
- [48] H. Gui, J. K. Streit, J. A. Fagan, A. R. Hight Walker, C. Zhou, M. Zheng, *Nano Lett.* **2015**, *15*, 1642.
- [49] B. Podlesny, T. Shiraki, D. Janas, *Sci. Rep.* **2020**, *10*, 9250.
- [50] a) J. A. Fagan, *Nanoscale Adv.* **2019**, *1*, 3307; b) E. Turek, T. Wasiak, G. Stando, D. Janas, *Nanotechnology* **2018**, *29*, 405704.
- [51] a) H. Tang, B. Wu, K. Chen, H. Pei, W. Wu, L. Ma, A. Peng, H. Ye, L. Chen, *J. Sep. Sci.* **2015**, *38*, 523; b) R. A. S. Cruz, H. Almeida, C. P. Fernandes, P. Joseph-Nathan, L. Rocha, G. G. Leitão, *J. Sep. Sci.* **2016**, *39*, 1273.
- [52] N. Mekaoui, K. Faure, A. Berthod, *Bioanalysis* **2012**, *4*, 833.
- [53] a) C. Han, J. Luo, Z. Li, Y. Zhang, H. Zhao, L. Kong, *J. Sep. Sci.* **2016**, *39*, 2413; b) S. Tong, X. Wang, M. Lu, Q. Xiong, Q. Wang, J. Yan, *J. Sep. Sci.* **2016**, *39*, 1567.
- [54] M. Zhang, C. Y. Khripin, J. A. Fagan, P. McPhie, Y. Ito, M. Zheng, *Anal. Chem.* **2014**, *86*, 3980.
- [55] M. Knight, R. Lazo-Portugal, S. N. Ahn, S. Stefansson, *J. Chromatogr. A* **2017**, *1483*, 93.

- [56] a) L. Luer, S. Hoseinkhani, D. Polli, J. Crochet, T. Hertel, G. Lanzani, *Nat. Phys.* **2009**, *5*, 54; b) F. Wang, G. Dukovic, L. E. Brus, T. F. Heinz, *Science* **2005**, *308*, 838.
- [57] a) S. Ren, M. Bernardi, R. R. Lunt, V. Bulovic, J. C. Grossman, S. Gradecak, *Nano Lett.* **2011**, *11*, 5316; b) E. Kymakis, G. A. J. Amaratunga, *Rev. Adv. Mater. Sci.* **2005**, *10*, 300.
- [58] a) D. J. Bindl, M. Y. Wu, F. C. Prehn, M. S. Arnold, *Nano Lett.* **2011**, *11*, 455; b) M. Gong, T. A. Shastry, Y. Xie, M. Bernardi, D. Jasion, K. A. Luck, T. J. Marks, J. C. Grossman, S. Ren, M. C. Hersam, *Nano Lett.* **2014**, *14*, 5308; c) A. Classen, L. Einsiedler, T. Heumueller, A. Graf, M. Brohmann, F. Berger, S. Kahmann, M. Richter, G. J. Matt, K. Forberich, J. Zaumseil, C. J. Brabec, *Adv. Energy Mater.* **2018**, *8*, 1801913.
- [59] M. Gong, T. A. Shastry, Q. Cui, R. R. Kohlmeier, K. A. Luck, A. Rowberg, T. J. Marks, M. F. Durstock, H. Zhao, M. C. Hersam, S. Ren, *ACS Appl. Mater. Interfaces* **2015**, *7*, 7428.
- [60] a) D. J. Bindl, M. J. Shea, M. S. Arnold, *Chem. Phys.* **2013**, *413*, 29; b) M. J. Shea, M. S. Arnold, *Appl. Phys. Lett.* **2013**, *102*, 243101.
- [61] D. D. Tune, J. G. Shapter, *Energy Environ. Sci.* **2013**, *6*, 2572.
- [62] a) R. D. Mehlenbacher, J. Wang, N. M. Kearns, M. J. Shea, J. T. Flach, T. J. McDonough, M. Y. Wu, M. S. Arnold, M. T. Zanni, *J. Phys. Chem. Lett.* **2016**, *7*, 2024; b) R. D. Mehlenbacher, T. J. McDonough, N. M. Kearns, M. J. Shea, Y. Joo, P. Gopalan, M. S. Arnold, M. T. Zanni, *J. Phys. Chem. C* **2016**, *120*, 17069; c) D. H. Arias, D. B. Sulas-Kern, S. M. Hart, H. S. Kang, J. Hao, R. Ihly, J. C. Johnson, J. L. Blackburn, A. J. Ferguson, *Nanoscale* **2019**, *11*, 21196.
- [63] J. T. Flach, J. Wang, M. S. Arnold, M. T. Zanni, *J. Phys. Chem. Lett.* **2020**, *11*, 6016.
- [64] T. A. Shastry, S. C. Clark, A. J. E. Rowberg, K. A. Luck, K. S. Chen, T. J. Marks, M. C. Hersam, *Adv. Energy Mater.* **2016**, *6*, 1501466.
- [65] D. J. Bindl, A. S. Brewer, M. S. Arnold, *Nano Res.* **2011**, *4*, 1174.
- [66] W. C. Tsoi, S. J. Spencer, L. Yang, A. M. Ballantyne, P. G. Nicholson, A. Turnbull, A. G. Shard, C. E. Murphy, D. D. C. Bradley, J. Nelson, J. S. Kim, *Macromolecules* **2011**, *44*, 2944.
- [67] J. Wang, S. R. Peurifoy, M. T. Bender, F. Ng, K.-S. Choi, C. Nuckolls, M. S. Arnold, *J. Phys. Chem. C* **2019**, *123*, 21395.
- [68] a) A. T. Mallajosyula, W. Nie, G. Gupta, J. L. Blackburn, S. K. Doorn, A. D. Mohite, *ACS Nano* **2016**, *10*, 10808; b) M. J. Shea, J. L. Wang, J. T. Flach, M. T. Zanni, M. S. Arnold, *APL Mater.* **2018**, *6*, 056104.
- [69] a) G. J. Brady, Y. Joo, S. S. Roy, P. Gopalan, M. S. Arnold, *Appl. Phys. Lett.* **2014**, *104*, 083107; b) H. Ozawa, N. Ide, T. Fujigaya, Y. Niidome, N. Nakashima, *Chem. Lett.* **2011**, *40*, 239.
- [70] S. L. Guillot, K. S. Mistry, A. D. Avery, J. Richard, A. M. Dowgiallo, P. F. Ndione, J. van de Lagemaat, M. O. Reese, J. L. Blackburn, *Nanoscale* **2015**, *7*, 6556.
- [71] a) R. M. Jain, R. Howden, K. Tvrđy, S. Shimizu, A. J. Hilmer, T. P. McNicholas, K. K. Gleason, M. S. Strano, *Adv. Mater.* **2012**, *24*, 4436; b) Z. Wu, Z. Chen, X. Du, J. M. Logan, J. Sippel, M. Nikolou, K. Kamaras, J. R. Reynolds, D. B. Tanner, A. F. Hebard, A. G. Rinzler, *Science* **2004**, *305*, 1273; c) X. He, W. Gao, L. Xie, B. Li, Q. Zhang, S. Lei, J. M. Robinson, E. H. Haroz, S. K. Doorn, W. Wang, R. Vajtai, P. M. Ajayan, W. W. Adams, R. H. Hauge, J. Kono, *Nat. Nanotechnol.* **2016**, *11*, 633.
- [72] C. M. Isborn, C. Tang, A. Martini, E. R. Johnson, A. Otero-de-la-Roza, V. C. Tung, *J. Phys. Chem. Lett.* **2013**, *4*, 2914.
- [73] Y. Joo, G. J. Brady, M. J. Shea, M. B. Oviedo, C. Kanimozhi, S. K. Schmitt, B. M. Wong, M. S. Arnold, P. Gopalan, *ACS Nano* **2015**, *9*, 10203.
- [74] N. F. Hartmann, R. Pramanik, A. M. Dowgiallo, R. Ihly, J. L. Blackburn, S. K. Doorn, *ACS Nano* **2016**, *10*, 11449.
- [75] R. D. Mehlenbacher, M. Y. Wu, M. Grechko, J. E. Laaser, M. S. Arnold, M. T. Zanni, *Nano Lett.* **2013**, *13*, 1495.
- [76] J. L. Wang, M. J. Shea, J. T. Flach, T. J. McDonough, A. J. Way, M. T. Zanni, M. S. Arnold, *J. Phys. Chem. C* **2017**, *121*, 8310.
- [77] a) A. M. Dowgiallo, K. S. Mistry, J. C. Johnson, O. G. Reid, J. L. Blackburn, *J. Phys. Chem. Lett.* **2016**, *7*, 1794; b) G. I. Koleilat, M. Vosgueritchian, T. Lei, Y. Zhou, D. W. Lin, F. Lissel, P. Lin, J. W. To, T. Xie, K. England, Y. Zhang, Z. Bao, *ACS Nano* **2016**, *10*, 11258.
- [78] M. Grechko, Y. Ye, R. D. Mehlenbacher, T. J. McDonough, M. Y. Wu, R. M. Jacobberger, M. S. Arnold, M. T. Zanni, *ACS Nano* **2014**, *8*, 5383.
- [79] a) C. Deibel, V. Dyakonov, *Rep. Prog. Phys.* **2010**, *73*, 096401; b) A. Wadsworth, Z. Hamid, J. Kosco, N. Gasparini, I. McCulloch, *Adv. Mater.* **2020**, *32*, 2001763.
- [80] B. C. Thompson, J. M. Frechet, *Angew. Chem., Int. Ed. Engl.* **2008**, *47*, 58.
- [81] Y. Ye, D. J. Bindl, R. M. Jacobberger, M. Y. Wu, S. S. Roy, M. S. Arnold, *Small* **2014**, *10*, 3299.
- [82] M. Schirowski, G. Abellan, E. Nuin, J. Pampel, C. Dolle, V. Wedler, T. P. Fellingner, E. Spiecker, F. Hauke, A. Hirsch, *J. Am. Chem. Soc.* **2018**, *140*, 3352.
- [83] S. Zeng, H. Chen, H. Wang, X. Tong, M. Chen, J. Di, Q. Li, *Small* **2017**, *13*, 1700518.
- [84] D. Landerer, C. Sprau, D. Baumann, P. Pingel, T. Leonhard, D. Zimmermann, C. L. Chochos, H. Kruger, S. Janietz, A. Colmann, *Sol. RRL* **2019**, *3*, 1800266.
- [85] A. Setaro, M. Adeli, M. Glaeske, D. Przyrembel, T. Bisswanger, G. Gordeev, F. Maschietto, A. Faghani, B. Paulus, M. Weinelt, R. Arenal, R. Haag, S. Reich, *Nat. Commun.* **2017**, *8*, 14281.
- [86] R. Ihly, K. S. Mistry, A. J. Ferguson, T. T. Clikeman, B. W. Larson, O. Reid, O. V. Boltalina, S. H. Strauss, G. Rumbles, J. L. Blackburn, *Nat. Chem.* **2016**, *8*, 603.
- [87] a) S. Li, L. Ye, W. Zhao, H. Yan, B. Yang, D. Liu, W. Li, H. Ade, J. Hou, *J. Am. Chem. Soc.* **2018**, *140*, 7159; b) W. Zhao, S. Li, H. Yao, S. Zhang, Y. Zhang, B. Yang, J. Hou, *J. Am. Chem. Soc.* **2017**, *139*, 7148; c) X. Liu, X. Li, Y. Zou, H. Liu, L. Wang, J. Fang, C. Yang, *J. Mater. Chem. A* **2019**, *7*, 3336.
- [88] A. Zhang, C. Xiao, D. Meng, Q. Wang, X. Zhang, W. Hu, X. Zhan, Z. Wang, R. A. J. Janssen, W. Li, *J. Mater. Chem. C* **2015**, *3*, 8255.
- [89] a) K. Yanagi, K. Iakoubovskii, H. Matsui, H. Matsuzaki, H. Okamoto, Y. Miyata, Y. Maniwa, S. Kazaoui, N. Minami, H. Kataura, *J. Am. Chem. Soc.* **2007**, *129*, 4992; b) A. Alam, S. Dehm, F. Hennrich, Y. Zakharko, A. Graf, M. Pfohl, I. M. Hossain, M. M. Kappes, J. Zaumseil, R. Krupke, B. S. Flavel, *Nanoscale* **2017**, *9*, 11205.
- [90] a) Y. Almadori, L. Alvarez, R. Le Parc, R. Aznar, F. Fossard, A. Loiseau, B. Joussemme, S. Campidelli, P. Hermet, A. Belhboub, A. Rahmani, T. Saito, J. L. Bantignies, *J. Phys. Chem. C* **2014**, *118*, 19462; b) Y. Almadori, G. Delport, R. Chambard, L. Orcin-Chaix, A. C. Selvati, N. Izard, A. Belhboub, R. Aznar, B. Joussemme, S. Campidelli, P. Hermet, R. Le Parc, T. Saito, Y. Sato, K. Suenaga, P. Puech, J. S. Lauret, G. Cassabois, J. L. Bantignies, L. Alvarez, *Carbon* **2019**, *149*, 772.
- [91] S. van Bezouw, D. H. Arias, R. Ihly, S. Cambre, A. J. Ferguson, J. Campo, J. C. Johnson, J. Defiliet, W. Wenseleers, J. L. Blackburn, *ACS Nano* **2018**, *12*, 6881.
- [92] S. Cambre, J. Campo, C. Beirnaert, C. Verlackt, P. Cool, W. Wenseleers, *Nat. Nanotechnol.* **2015**, *10*, 248.
- [93] a) N. Murakami, H. Miyake, T. Tajima, K. Nishikawa, R. Hirayama, Y. Takaguchi, *J. Am. Chem. Soc.* **2018**, *140*, 3821; b) Y. Takaguchi, H. Miyake, T. Izawa, D. Miyamoto, R. Sagawa, T. Tajima, *Phosphorus Sulfur* **2019**, *194*, 707.
- [94] a) T. Yan, W. Song, J. Huang, R. Peng, L. Huang, Z. Ge, *Adv. Mater.* **2019**, *31*, 1902210; b) Y. Lin, B. Adilbekova, Y. Firdaus, E. Yengel, H. Faber, M. Sajjad, X. Zheng, E. Yarali, A. Seitkhan, O. M. Bakr, A. El-Labban, U. Schwingenschlöggl, V. Tung, I. McCulloch, F. Laqui, T. D. Anthopoulos, *Adv. Mater.* **2019**, *31*, 1902965; c) Q. Liu, Y. Jiang, K. Jin, J. Qin, J. Xu, W. Li, J. Xiong, J. Liu,

- Z. Xiao, K. Sun, S. Yang, X. Zhang, L. Ding, *Sci. Bull.* **2020**, *65*, 272; d) M. Nakamura, K. Yamaguchi, Y. Kimoto, Y. Yasaki, T. Kato, H. Sugimoto, *IEEE J. Photovoltaics* **2019**, *9*, 1863; e) M. A. Green, E. D. Dunlop, J. Hohl-Ebinger, M. Yoshita, N. Kopidakis, A. W. Y. Ho-Baillie, *Prog. Photovoltaics* **2020**, *28*, 3.
- [95] K. E. Moore, B. S. Flavel, A. V. Ellis, J. G. Shapter, *Carbon* **2011**, *49*, 2639.
- [96] a) S. N. Habisreutinger, T. Leijtens, G. E. Eperon, S. D. Stranks, R. J. Nicholas, H. J. Snaith, *Nano Lett.* **2014**, *14*, 5561; b) S. N. Habisreutinger, T. Leijtens, G. E. Eperon, S. D. Stranks, R. J. Nicholas, H. J. Snaith, *J. Phys. Chem. Lett.* **2014**, *5*, 4207.
- [97] M. A. Contreras, T. Barnes, J. van de Lagemaat, G. Rumbles, T. J. Coutts, C. Weeks, P. Glatkowski, I. Levitsky, J. Peltola, D. A. Britz, *J. Phys. Chem. C* **2007**, *111*, 14045.
- [98] a) T. M. Barnes, X. Wu, J. Zhou, A. Duda, J. van de Lagemaat, T. J. Coutts, C. L. Weeks, D. A. Britz, P. Glatkowski, *Appl. Phys. Lett.* **2007**, *90*, 243503; b) A. B. Phillips, R. R. Khandal, Z. Song, R. M. Zartman, J. L. DeWitt, J. M. Stone, P. J. Rohan, V. V. Plotnikov, C. W. Carter, J. M. Stayancho, R. J. Ellingson, A. D. Compaan, M. J. Heben, *Nano Lett.* **2013**, *13*, 5224.
- [99] a) J. van de Lagemaat, T. M. Barnes, G. Rumbles, S. E. Shaheen, T. J. Coutts, C. Weeks, I. Levitsky, J. Peltola, P. Glatkowski, *Appl. Phys. Lett.* **2006**, *88*, 233503; b) T. M. Barnes, J. D. Bergeson, R. C. Tenent, B. A. Larsen, G. Teeter, K. M. Jones, J. L. Blackburn, J. van de Lagemaat, *Appl. Phys. Lett.* **2010**, *96*, 243309; c) M. W. Rowell, M. A. Topinka, M. D. McGehee, H.-J. Prall, G. Dennler, N. S. Sariciftci, L. Hu, G. Gruner, *Appl. Phys. Lett.* **2006**, *88*, 233506; d) A. D. Pasquier, H. E. Unalan, A. Kanwal, S. Miller, M. Chhowalla, *Appl. Phys. Lett.* **2005**, *87*, 203511.
- [100] G. D. M. R. Dabera, K. D. G. I. Jayawardena, M. R. R. Prabhath, I. Yahya, Y. Y. Tan, N. A. Nismy, H. Shiozawa, M. Sauer, G. Ruiz-Soria, P. Ayala, V. Stolojan, A. A. D. T. Adikaari, P. D. Jarowski, T. Pichler, S. R. P. Silva, *ACS Nano* **2013**, *7*, 556.
- [101] R. Ihly, A.-M. Dowgiallo, M. Yang, P. Schulz, N. J. Stanton, O. G. Reid, A. J. Ferguson, K. Zhu, J. J. Berry, J. L. Blackburn, *Energy Environ. Sci.* **2016**, *9*, 1439.
- [102] K. Aitola, K. Domanski, J.-P. Correa-Baena, K. Sveinbjörnsson, M. Saliba, A. Abate, M. Grätzel, E. Kauppinen, E. M. J. Johansson, W. Tress, A. Hagfeldt, G. Boschloo, *Adv. Mater.* **2017**, *29*, 1606398.
- [103] S. N. Habisreutinger, N. K. Noel, B. W. Larson, O. G. Reid, J. L. Blackburn, *ACS Energy Lett.* **2019**, *4*, 1872.
- [104] I. Jeon, A. Shawky, S. Seo, Y. Qian, A. Anisimov, E. I. Kauppinen, Y. Matsuo, S. Maruyama, *J. Mater. Chem. A* **2020**, *8*, 11141.
- [105] I. Jeon, S. Seo, Y. Sato, C. Delacou, A. Anisimov, K. Suenaga, E. I. Kauppinen, S. Maruyama, Y. Matsuo, *J. Phys. Chem. C* **2017**, *121*, 25743.
- [106] T. G. Allen, J. Bullock, X. Yang, A. Javey, S. De Wolf, *Nat. Energy* **2019**, *4*, 914.
- [107] a) A. K. Jena, A. Kulkarni, T. Miyasaka, *Chem. Rev.* **2019**, *119*, 3036; b) R. Mohan, R. Paulose, *Photoenergy and Thin Film Materials* (Ed: X.-Y. Yang), Scrivener Publishing LLC **2019**, pp. 157–192; c) R. Xue, J. Zhang, Y. Li, Y. Li, *Small* **2018**, *14*, 1801793.
- [108] A. Richter, M. Hermle, S. W. Glunz, *IEEE J. Photovoltaics* **2013**, *3*, 1184.
- [109] A. Blakers, *IEEE J. Photovoltaics* **2019**, *9*, 629.
- [110] a) C. Battaglia, A. Cuevas, S. De Wolf, *Energy Environ. Sci.* **2016**, *9*, 1552; b) K. Yoshikawa, W. Yoshida, T. Irie, H. Kawasaki, K. Konishi, H. Ishibashi, T. Asatani, D. Adachi, M. Kanematsu, H. Uzu, *Sol. Energy Mater. Sol.* **2017**, *173*, 37.
- [111] T. Tiedje, E. Yablonovitch, G. D. Cody, B. G. Brooks, *IEEE Trans. Electron Devices* **1984**, *31*, 711.
- [112] M. J. Kerr, A. Cuevas, *Semicond. Sci. Technol.* **2002**, *17*, 35.
- [113] B. Liao, R. Stangl, T. Mueller, F. Lin, C. S. Bhatia, B. Hoex, *J. Appl. Phys.* **2013**, *113*, 024509.
- [114] S. Ardali, G. Atmaca, S. Lisesivdin, T. Malin, V. Mansurov, K. Zhuravlev, E. Tiras, *Phys. Status Solid B* **2015**, *252*, 1960.
- [115] S. De Wolf, M. Kondo, *Appl. Phys. Lett.* **2007**, *90*, 042111.
- [116] A. Moehlecke, T. L. Marcondes, J. d. Aquino, I. Zanesco, M. Ly, *Mater. Res.* **2020**, *23*, e20190536.
- [117] S. M. De Nicolás, D. Muñoz, A. Ozanne, N. Nguyen, P. Ribeyron, *Energy Procedia* **2011**, *8*, 226.
- [118] H. Ali, H. A. Khan, *Int. Trans. Electr. Energy Sys.* **2020**, *30*, 12351.
- [119] G. Coletti, S. L. Luxembourg, L. J. Geerligs, V. Rosca, A. R. Burgers, Y. Wu, L. Okel, M. Kloos, F. J. K. Danzl, M. Najafi, D. Zhang, I. Dogan, V. Zardetto, F. Di Giacomo, J. Kroon, T. Aernouts, J. Huepkes, C. H. Burgess, M. Creatore, R. Andriessen, S. Veenstra, *ACS Energy Lett.* **2020**, *5*, 1676.
- [120] a) J. Bullock, M. Hettick, J. Geissbuhler, A. J. Ong, T. Allen, C. M. Sutter-Fella, T. Chen, H. Ota, E. W. Schaler, S. De Wolf, C. Ballif, A. Cuevas, A. Javey, *Nat. Energy* **2016**, *1*, 15031; b) S. Murase, Y. Yang, *Adv. Mater.* **2012**, *24*, 2459; c) J. He, P. Gao, Z. Yang, J. Yu, W. Yu, Y. Zhang, J. Sheng, J. Ye, J. C. Amine, Y. Cui, *Adv. Mater.* **2017**, *29*, 1606321.
- [121] Y. Zhang, F. Zu, S. T. Lee, L. Liao, N. Zhao, B. Sun, *Adv. Energy Mater.* **2014**, *4*, 1300923.
- [122] Y. Zhang, W. Cui, Y. Zhu, F. Zu, L. Liao, S. Lee, B. Sun, *Energy Environ. Sci.* **2015**, *8*, 927.
- [123] a) C. Battaglia, X. Yin, M. Zheng, I. D. Sharp, T. Chen, S. McDonnell, A. Azcatl, C. Carraro, B. Ma, R. Maboudian, *Nano Lett.* **2014**, *14*, 967; b) J. Geissbühler, J. Werner, S. Martin de Nicolas, L. Barraud, A. Hessler-Wyser, M. Despeisse, S. Nicolay, A. Tomasi, B. Niesen, S. De Wolf, *Appl. Phys. Lett.* **2015**, *107*, 081601; c) J. Dréon, Q. Jeangros, J. Cattin, J. Haschke, L. Antognini, C. Ballif, M. Boccard, *Nano Energy* **2020**, *70*, 104495.
- [124] a) J. Chen, D. D. Tune, K. Ge, H. Li, B. S. Flavel, *Adv. Funct. Mater.* **2020**, *30*, 2000484; b) J. M. Harris, R. J. Headrick, M. R. Semler, J. A. Fagan, M. Pasquali, E. K. Hobbie, *Nanoscale* **2016**, *8*, 7969; c) J. M. Harris, M. R. Semler, S. May, J. A. Fagan, E. K. Hobbie, *J. Phys. Chem. C* **2015**, *119*, 10295; d) K. Cui, Y. Qian, I. Jeon, A. Anisimov, Y. Matsuo, E. I. Kauppinen, S. Maruyama, *Adv. Energy Mater.* **2017**, *7*, 1700449.
- [125] a) I. Jeon, J. Yoon, U. Kim, C. Lee, R. Xiang, A. Shawky, J. Xi, J. Byeon, H. M. Lee, M. Choi, S. Maruyama, Y. Matsuo, *Adv. Energy Mater.* **2019**, *9*, 1901204; b) Y. Kuwahara, T. Hirai, T. Saito, *J. Nanomater.* **2018**, *2018*, 5393290.
- [126] J. Wei, Y. Jia, Q. Shu, Z. Gu, K. Wang, D. Zhuang, G. Zhang, Z. Wang, J. Luo, A. Cao, *Nano Lett.* **2007**, *7*, 2317.
- [127] a) Y. Jia, P. Li, X. Gui, J. Wei, K. Wang, H. Zhu, D. Wu, L. Zhang, A. Cao, Y. Xu, *Appl. Phys. Lett.* **2011**, *98*, 133115; b) X. Li, Y. Jung, K. Sakimoto, T.-H. Goh, M. A. Reed, A. D. Taylor, *Energy Environ. Sci.* **2013**, *6*, 879; c) H. Wu, X. Zhao, Y. Wu, Q. Ji, L. Dai, Y. Shang, A. Cao, *Nano Res.* **2020**, *13*, 543.
- [128] a) K. Yoshikawa, H. Kawasaki, W. Yoshida, T. Irie, K. Konishi, K. Nakano, T. Uto, D. Adachi, M. Kanematsu, H. Uzu, *Nat. Energy* **2017**, *2*, 17032; b) S. De Wolf, A. Descoedres, Z. C. Holman, C. Ballif, *Green* **2012**, *2*, 7.
- [129] D. D. Tune, A. J. Blanch, R. Krupke, B. S. Flavel, J. G. Shapter, *Phys. Status Solidi A* **2014**, *217*, 1479.
- [130] L. Hu, D. Hecht, G. Grüner, *Nano Lett.* **2004**, *4*, 2513.
- [131] H.-Z. Geng, K. K. Kim, K. P. So, Y. S. Lee, Y. Chang, Y. H. Lee, *J. Am. Chem. Soc.* **2007**, *129*, 7758.
- [132] a) S. Ramesh, L. M. Ericson, V. A. Davis, R. K. Saini, C. Kittrell, M. Pasquali, W. Billups, W. W. Adams, R. H. Hauge, R. E. Smalley, *J. Phys. Chem. B* **2004**, *108*, 8794; b) D. D. Tune, A. J. Blanch, C. J. Shearer, K. E. Moore, M. Pfohl, J. G. Shapter, B. S. Flavel, *ACS Appl. Mater. Interfaces* **2015**, *7*, 25857.
- [133] K. K. Kim, J. J. Bae, H. K. Park, S. M. Kim, H.-Z. Geng, K. A. Park, H.-J. Shin, S.-M. Yoon, A. Benayad, J.-Y. Choi, *J. Am. Chem. Soc.* **2008**, *130*, 12757.
- [134] a) U. Dettlaff-Weglikowska, V. Skákalová, R. Graupner, S. H. Jhang, B. H. Kim, H. J. Lee, L. Ley, Y. W. Park, S. Berber, D. Tománek,

- J. Am. Chem. Soc.* **2005**, *127*, 5125; b) D. D. Tune, H. Shirae, V. Lami, R. J. Headrick, M. Pasquali, Y. Vaynzof, S. Noda, E. K. Hobbie, B. S. Flavel, *ACS Appl. Energy Mater.* **2019**, *2*, 5925; c) D. D. Tune, B. S. Flavel, J. S. Quinton, A. V. Ellis, J. G. Shapter, *ChemSusChem* **2013**, *6*, 320.
- [135] B. J. Landi, R. P. Raffaele, M. J. Heben, J. L. Alleman, W. VanDerveer, T. Gennett, *Nano Lett.* **2002**, *2*, 1329.
- [136] Y. Qian, I. Jeon, Y. L. Ho, C. Lee, S. Jeong, C. Delacou, S. Seo, A. Anisimov, E. I. Kauppinen, Y. Matsuo, *Adv. Energy Mater.* **2020**, *10*, 1902389.
- [137] H. Hanaei, M. K. Assadi, R. Saidur, *Renewable Sustainable Energy Rev.* **2016**, *59*, 620.
- [138] L. Yu, M. Batmunkh, M. Dadkhah, C. J. Shearer, J. G. Shapter, *Energy Environ. Mater.* **2018**, *1*, 232.
- [139] a) J. Chen, Y. Shen, J. Guo, B. Chen, J. Fan, F. Li, H. Liu, Y. Xu, Y. Mai, *Appl. Phys. Lett.* **2017**, *110*, 083904; b) J. Chen, K. Ge, C. Zhang, J. Guo, L. Yang, D. Song, F. Li, Z. Xu, Y. Xu, Y. Mai, *ACS Appl. Mater. Interfaces* **2018**, *10*, 44890.
- [140] A. Descoedres, L. Barraud, S. De Wolf, B. Strahm, D. Lachenal, C. Guérin, Z. Holman, F. Zicarelli, B. Demareux, J. Seif, *Appl. Phys. Lett.* **2011**, *99*, 123506.
- [141] a) L. Wan, C. Zhang, K. Ge, X. Yang, F. Li, W. Yan, Z. Xu, L. Yang, Y. Xu, D. Song, *Adv. Energy Mater.* **2020**, *10*, 1903851; b) J. Chen, D. D. Tune, K. Ge, H. Li, B. S. Flavel, *Adv. Funct. Mater.* **2020**, *30*, 2000484.
- [142] a) J. Chen, K. Ge, B. Chen, J. Guo, L. Yang, Y. Wu, G. Coletti, H. Liu, F. Li, D. Liu, *Sol. Energy Mater. Sol.* **2019**, *195*, 99; b) J. Chen, Y. Shen, J. Guo, B. Chen, J. Fan, F. Li, B. Liu, H. Liu, Y. Xu, Y. Mai, *Electrochim. Acta* **2017**, *247*, 826; c) J. Chen, B. Chen, Y. Shen, J. Guo, B. Liu, X. Dai, Y. Xu, Y. Mai, *Appl. Phys. Lett.* **2017**, *111*, 191601.
- [143] L. Yang, J. Guo, J. Li, J. Yan, K. Ge, J. Jiang, H. Li, *J. Mater. Chem. C* **2020**, <https://doi.org/10.1039/d0tc03384g>.
- [144] a) J. Chen, L. Wan, H. Li, J. Yan, J. Ma, B. Sun, F. Li, B. S. Flavel, *Adv. Funct. Mater.* **2020**, *30*, 2004476; b) D. D. Tune, N. Mallik, H. Fornasier, B. S. Flavel, *Adv. Energy Mater.* **2020**, *10*, 1903261.
- [145] X. Ru, M. Qu, J. Wang, T. Ruan, M. Yang, F. Peng, W. Long, K. Zheng, H. Yan, X. Xu, *Sol. Energy Mater. Sol.* **2020**, *215*, 110643.
- [146] J. Zhu, X. Yang, Z. Yang, D. Wang, P. Gao, J. Ye, *Adv. Funct. Mater.* **2018**, *28*, 1705425.
- [147] A. Javey, H. Kim, M. Brink, Q. Wang, A. Ural, J. Guo, P. McIntyre, P. McEuen, M. Lundstrom, H. Dai, *Nat. Mater.* **2002**, *1*, 241.
- [148] B. Singha, C. S. Solanki, *Mater. Res. Express* **2017**, *4*, 072001.
- [149] F. Feldmann, M. Simon, M. Bivour, C. Reichel, M. Hermle, S. W. Glunz, *Sol. Energy Mater. Sol.* **2014**, *131*, 100.
- [150] a) A. Richter, J. Benick, R. Müller, F. Feldmann, C. Reichel, M. Hermle, S. W. Glunz, *Prog. Photovoltaics* **2018**, *26*, 579; b) X. Yang, Q. Bi, H. Ali, K. Davis, W. V. Schoenfeld, K. Weber, *Adv. Mater.* **2016**, *28*, 5891; c) X. Yang, Y. Lin, J. Liu, W. Liu, Q. Bi, X. Song, J. Kang, F. Xu, L. Xu, M. N. Hedhili, *Adv. Mater.* **2020**, *32*, 2002608.
- [151] a) J. Bullock, Y. M. Wan, Z. R. Xu, S. Essig, M. Hettick, H. C. Wang, W. B. Ji, M. Boccard, A. Cuevas, C. Ballif, A. Javey, *ACS Energy Lett.* **2018**, *3*, 508; b) S. H. Zhong, J. Dreon, Q. Jeangros, E. Aydin, S. De Wolf, F. Fu, M. Boccard, C. Ballif, *Adv. Funct. Mater.* **2019**, *30*, 1907840.
- [152] a) S. Schneider, M. Brohmann, R. Lorenz, Y. J. Hofstetter, M. Rother, E. Sauter, M. Zharnikov, Y. Vaynzof, H.-J. Himmell, J. Zaumseil, *ACS Nano* **2018**, *12*, 5895; b) L. Brownlie, J. Shapter, *Carbon* **2018**, *126*, 257.
- [153] Y. Jung, X. Li, N. K. Rajan, A. D. Taylor, M. A. Reed, *Nano Lett.* **2013**, *13*, 95.
- [154] D. Zielke, R. Gogolin, M. U. Halbich, C. Marquardt, W. Lövenich, R. Sauer, J. Schmidt, *Sol. RRL* **2018**, *2*, 1700191.
- [155] K. Ellmer, *Nat. Photonics* **2012**, *6*, 809.
- [156] X. G. Hu, P. X. Hou, J. B. Wu, X. Li, J. Luan, C. Liu, G. Liu, H. M. Cheng, *Nano Energy* **2020**, *69*, 104442.
- [157] a) I. Jeon, C. Delacou, H. Okada, G. E. Morse, T. H. Han, Y. Sato, A. Anisimov, K. Suenaga, E. I. Kauppinen, S. Maruyama, Y. Matsuo, *J. Mater. Chem. A* **2018**, *6*, 14553; b) S. J. Kwon, T. H. Han, T. Y. Ko, N. Li, Y. Kim, D. J. Kim, S. H. Bae, Y. Yang, B. H. Hong, K. S. Kim, S. Ryu, T. W. Lee, *Nat. Commun.* **2018**, *9*, 2037.



Laura Wieland is a Ph.D. student enrolled at the Technical University Darmstadt and has been a member of the Flavel research group since 2018. She holds a Bachelor degree in chemistry from the Ruprecht Karl University of Heidelberg and a Masters from the Karlsruhe Institute of Technology. Her research interests include the integration of SWCNT films in organic solar cells and optimization of light absorption by endohedral functionalization with dyes.



Jianhui Chen joined Hebei University in 2014, obtained his Ph.D. there in 2017 and is currently an assistant professor. His research interests include organic–inorganic interface physics, organic passivation strategies for silicon solar cells, low-dimensional/organic composite materials and organic–inorganic hybrid interface memories. Since 2018 he is a China Scholarship Council fellow at the Karlsruhe Institute of Technology, where he works to apply polymer passivation to carbon nanotube silicon solar cells.



Benjamin S. Flavel obtained both a B.Sc. (Hons) and Ph.D. in Nanotechnology at the Flinders University of South Australia and completed a Habilitation in Materials Science at the Technical University Darmstadt. He has received research fellowships from the Australian Government's Endeavour Program, the Alexander von Humboldt Foundation and is the recipient of both the Emmy Noether and Heisenberg programs from the German Research Foundation (DFG). He is currently a Group Leader at the Institute of Nanotechnology, Karlsruhe Institute of Technology where he pursues his research interests of carbon nanotube separation and their integration into devices for optics, electronics, and energy.